



저작자표시-비영리-변경금지 2.0 대한민국

이용자는 아래의 조건을 따르는 경우에 한하여 자유롭게

- 이 저작물을 복제, 배포, 전송, 전시, 공연 및 방송할 수 있습니다.

다음과 같은 조건을 따라야 합니다:



저작자표시. 귀하는 원저작자를 표시하여야 합니다.



비영리. 귀하는 이 저작물을 영리 목적으로 이용할 수 없습니다.



변경금지. 귀하는 이 저작물을 개작, 변형 또는 가공할 수 없습니다.

- 귀하는, 이 저작물의 재이용이나 배포의 경우, 이 저작물에 적용된 이용허락조건을 명확하게 나타내어야 합니다.
- 저작권자로부터 별도의 허가를 받으면 이러한 조건들은 적용되지 않습니다.

저작권법에 따른 이용자의 권리는 위의 내용에 의하여 영향을 받지 않습니다.

이것은 [이용허락규약\(Legal Code\)](#)을 이해하기 쉽게 요약한 것입니다.

[Disclaimer](#)

August 2019

Doctor's Degree Thesis

SIR Evaluation of FSDT Human Body Communication and Its Application for WLAN Service

Graduate School of Chosun University

Department of IT Fusion Technology

Kunho Park

SIR Evaluation of FSDT Human Body Communication and Its Application for WLAN Service

FSDT 인체통신의 SIR 성능 평가 및 WLAN 서비스를 위한
어플리케이션

August 23, 2019

Graduate School of Chosun University
Department of IT Fusion Technology
Kunho Park

SIR Evaluation of FSDT Human Body Communication and Its Application for WLAN Service

Advisor : Prof. Youn Tae Kim

This thesis is submitted to The Graduate School of
Chosun University in partial fulfillment of the
requirements for the Doctor's degree

April 2019

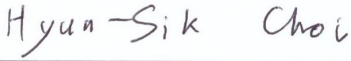
Graduate School of Chosun University
Department of IT Fusion Technology
Kunho Park

This is to certify that the Doctor's Thesis of Kunho Park

has been approved by the Examining Committee for the thesis
requirement for the Doctor's degree in IT Fusion Technology

Committee Chairperson
Prof. Keun-Chang Kwak  (Sign)

Committee Member
Dr. Jung Hwan Hwang  (Sign)

Committee Member
Prof. Hyun-Sik Choi  (Sign)

Committee Member
Prof. Eun Seo Choi  (Sign)

Committee Member
Prof. Youn Tae Kim  (Sign)

June 2019

Graduate School of Chosun University

Table of Contents

Table of Contents	i
List of Tables	iii
List of Figures	iv
Acronyms	vi
Abstract(Korean)	viii
Abstract(English)	x
I. Introduction	1
II. Performance evaluation of human body communication using FSDT	4
A. Analysis of human body channel characteristics	4
1. Measurement setup for analysis of body channel characteristics	5
2. Measurement results of body channel characteristics ..	9
A) Signal loss characteristics	9
B) Time delay characteristics	12
3. Correlation characteristics	16
A) Correlation between signal loss and body characteristics ·	19
B) Correlation between time delay and body characteristics ·	23
C) Analysis of correlation characteristics	27
B. Analysis of BER performance	30
1. Measurement setup for BER performance	30
A) Measurement setup for BER vs. Interference frequency ·	31

B) Measurement setup for BER vs. SIR	34
2. Performance and test results	36
A) Receiver	36
B) BER versus interference frequency	37
C) BER versus SIR	39
III. Touch-based dual-transmission system	43
A. Applications of human body communication	43
B. System configuration of dual-transmission application system	48
1. Physical signaling	48
2. Network setup	50
3. Data transfer	53
4. System configuration	54
C. Performance evaluation of dual-transmission application system	55
IV. Conclusion	58
References	61
List of Publications	65

List of Tables

Table 2.1	Subjects for human body channel analysis	5
Table 2.2	Average and standard deviation of signal loss by weight of experimental group	19
Table 2.3	Average and standard deviation of signal loss by muscle of experimental group	20
Table 2.4	Average and standard deviation of signal loss by fat mass of experimental group	20
Table 2.5	Average and standard deviation of signal loss by total body water of experimental group	20
Table 2.6	Correlation coefficient of signal loss according to body characteristics	22
Table 2.7	Average and standard deviation of time delay by weight of experimental group	24
Table 2.8	Average and standard deviation of time delay by muscle of experimental group	24
Table 2.9	Average and standard deviation of time delay by fat mass of experimental group	24
Table 2.10	Average and standard deviation of time delay by total body water of experimental group	25
Table 2.11	Correlation coefficient of time delay according to body characteristics	27
Table 2.12	Correlation coefficient between body characteristics ..	29
Table 2.13	Performance comparison with conventional body channel transceiver	41
Table 3.1	Comparison of TBCDT service with various communication services	45
Table 3.2	Specifications of HBC module	48

List of Figures

Figure 2.1	Diagram of channel model transmitter and receiver · 5
Figure 2.2	(left) Patch type, (right) watch type channel modeling transmitter 6
Figure 2.3	(left) Patch type, (right) watch type channel modeling receiver 7
Figure 2.4	(left) Measurement setup of body characteristics, (right) measurement setup for impulse response characteristics 7
Figure 2.5	Figure 2.5 Measurement setup for impulse response characteristics (left) patch to watch, (right) watch to patch 8
Figure 2.6	(a) Output signal of patch type receiver, (b) output signal of watch type receiver 9
Figure 2.7	Signal loss (a) patch to watch, (b) watch to patch 10
Figure 2.8	Power delay profile (a) patch to watch, (b) watch to patch 13
Figure 2.9	Mean delay (a) patch to watch, (b) watch to patch 14
Figure 2.10	RMS delay (a) patch to watch, (b) watch to patch ... 15
Figure 2.11	(a) Weight, (b) muscle, (c) fat mass, (d) total body water analysis graph for the experimental group ... 16
Figure 2.12	Correlation scatter diagram of signal loss according to body characteristics (a) weight, (b) muscle, (c) fat mass, (d) total body water, (e) RMS delay 21
Figure 2.13	Correlation scatter diagram of time delay according to body characteristics (a) weight, (b) muscle, (c) fat

	mass, (d) total body water	25
Figure 2.14	Correlation scatter diagram between body characteristics (a) weight-muscle, (b) weight-fat mass, (c) weight-height	29
Figure 2.15	Diagram of measurement setup for BER evaluation according to the interference frequency	31
Figure 2.16	(a) Received signal at Rx1 in Figure 1, (b) signal and interference power of the received signal	33
Figure 2.17	Diagram of measurement setup for BER evaluation according to the interference power	34
Figure 2.18	HBC receiver and differential to single circuitry	37
Figure 2.19	BER measurements under in-band and out-of-band interference of HBC	38
Figure 2.20	BER performance of the proposed FSĐT receiver module at out-of-band of 80 MHz	39
Figure 2.21	BER performance of the proposed FSĐT receiver module at in-band interference of 15 MHz	40
Figure 3.1	Touch-based dual-transmission communication system diagram	44
Figure 3.2	Touch-based dual-transmission communication service coverage area	47
Figure 3.3	Metal electrode HBC module and transparent electrode HBC module	49
Figure 3.4	Network layer state diagram	50
Figure 3.5	(a) Network setup, (b) Data transmission ladder diagram	51
Figure 3.6	Scenario flow chart	56
Figure 3.7	Touch-based dual-transmission communication service demonstration	57

Acronyms

WBAN	Wireless Body Area Network
HBC	Human Body Communication
PDP	Power Delay Profile
RMS	Root Mean Square
FSDT	Frequency Selective Digital Transmission
BER	Bit Error Rate
SIR	Signal to Interference Ratio
AFH	Adaptive Frequency Hopping
NRZ	Non Return to Zero
TBDT	Touch Based Dual Transmission

WiMAX	Worldwide Interoperability for microwave access
UWB	Ultra-Wide Band
AFE	Analog Front End
FPGA	Field Programable Gate Array
USB	Universal Serial Bus
TDD	Time-Division Duplex
ACQ	Acquisition
WLAN	Wireless Local Area Network
ISI	Inter-symbol Interference
PSD	Power Spectral Density
Wi-Fi	Wireless-Fidelity

요 약

FSDT 인체통신의 SIR 성능 평가 및 WLAN를 위한 어플리케이션

박건호

지도교수 : 김운태, Ph. D.

조선대학교 대학원, IT 융합학과

이 논문은 주파수 선택적 디지털 전송방식(FSDT)을 사용하는 인체통신(HBC)을 위한 인체 채널의 특성 및 주변 환경에 따른 수신 성능을 분석하고, 이 채널을 사용하는 인체통신 모듈의 성능 평가 및 이를 활용하는 멀티미디어 제공 시스템을 제시한다.

인체통신 기술은 안테나역할을 하는 인체 채널을 사용하기 때문에 인체 채널의 특성과 사용자의 주변 환경에 따라 통신 모듈의 수신 성능에 큰 영향을 받는다. 이러한 인체 채널의 신호 전달 특성을 분석하기 위해 120명의 성인 남성의 인체 채널을 통해 수신신호를 측정하여 분석하였다. 인체 채널의 수신신호 특성은 가슴에서 손목으로 송신했을 경우 주파수별 평균 신호 손실은 -65 dB, 표준편차는 2.35 dB이고, 손목에서 가슴으로 송신했을 경우 평균 신호 손실은 -64 dB, 표준편차는 2.65 dB를 보여주었다. 또한, 인체 채널의 특성을 체중 및 골격근량, 체지방량, 체수분량과 송수신 방향 신호 손실과의 상관관계를 구하였다.

이러한 인체 채널에서 FSDT 방식을 사용하는 인체통신 모듈의 배경간섭 신호에 대한 Bit error rate(BER) 특성을 분석하였다. 인체에 큰 영향을 끼치는 주파수 대역인 FM 라디오 주파수 대역의 1-100 MHz의 간섭신호를 -2.54 dB의 Signal to interference ratio(SIR)을 갖는 간섭신호를 채널에 인가하였다. 인체채널의 감쇄특성은 120명의 피실험자를 대상으로 측정함

평균신호손실을 고려하여 측정셋업을 구성하였다.

인체통신 모듈의 In-band 대역인 15 MHz 대역에서 BER은 10^{-3} 이하의 에러율을 보여주었고, Out-of-band 대역에서는 10^{-4} 이하의 에러율을 보여주었다. FSDT 방식은 다른 인체통신 기술에서 사용되는 모듈레이션 방식에 비해 100배 이상의 낮은 에러율을 갖는 것을 확인할 수 있었다. 이러한 성능 분석을 통해 FSDT 방식을 사용하는 인체통신 모듈이 인체통신 기술에 매우 적합하다는 것을 확인할 수 있었다.

또한 낮은 에러율을 갖는 FSDT 방식을 사용하는 인체통신 기술과 Wireless local area network(WLAN) 기술을 결합하여 고용량의 멀티미디어 데이터를 전송할 수 있는 접촉기반 이중 전송(TBDT) 서비스 시스템을 제안하였다. 이 시스템은 인체통신 기술을 통해 디바이스와 디바이스의 네트워크를 연결하고, WLAN을 통해 고용량 데이터를 고속으로 전송할 수 있는 시스템이다. 이 시스템은 인체통신을 활용한 어플리케이션의 일환으로 직관적이고 간편한 서비스를 제공할 수 있을 것으로 예상된다.

Abstract

SIR Evaluation of FSDT Human Body Communication and Its Application for WLAN Service

Kunho Park

Advisor : Prof. Youn Tae Kim, Ph.D.

Department of IT Fusion Technology,

Graduate School of Chosun University

In this thesis, we analyze the characteristics of the body channel and the reception performance according to the surrounding environment of human body communication(HBC) technology using frequency selective digital transmission(FSDT) technology. We evaluate the performance of HBC module using this channel and present a multimedia service system that utilizes HBC.

Because the human body acts as an antenna, the HBC is influenced by the human channel and the user's surroundings. To analyze the signal transmission characteristics of the human channel, the received signals were measured and analyzed through human channels of 120 adult males.

The average signal loss of the human channel is -65 dB and the standard deviation is 2.35 dB when transmitted from the chest to the wrist. The average signal loss when transmitting from the wrist to the

chest was -64 dB and the standard deviation was 2.65 dB. In addition, the correlation between human body channel characteristics and body weight, skeletal muscle mass, body fat mass, total body water and transmission / reception direction signal loss were obtained.

The signal to interference ratio(SIR) of the human body channel is obtained by the bit error rate(BER) of the HBC module using the FSDT method. An interference signal of $1-100$ MHz in the FM radio frequency band, which has a large influence on the human body, and an interference signal of -2.54 dB in SIR are applied to the channel. The attenuation characteristics of the human channel were constructed by considering the average signal loss measured in 120 subjects. In the in-band 15 MHz band of the HBC module, the BER showed an error rate of 10^{-3} or less, and in the out-of-band, the error rate was 10^{-4} or less. The FSDT method has a low error rate of 100 times or more as compared with the another modulation methods. Through this performance analysis, we can confirm that HBC module using FSDT method is very suitable for HBC.

A touch-based dual-transmission(TBDT) system in which HBC and wireless local area network(WLAN) are combined to provide an intuitive service, is proposed. This system connects devices and network of devices through HBC, and can transmit high capacity data at high speed through WLAN. The system is expected to provide intuitive and simple services as part of applications utilizing HBC.

I. Introduction

HBC has been proposed as a communication technology for a body area network(BAN), in which wearable devices communicate with each other or with peripheral devices [1]. In particular, the sensor network technology has recently been applied to the human body related fields, and the sensor network is being developed around the human body to provide the human body health service. HBC does not have a cable between devices, so it satisfies portability and convenience. Because HBC can be intuitively networked through simple contact, user-oriented service provision can be easily implemented. In addition, low power consumption and high data transmission characteristics are applicable to various fields such as wearable devices and medical devices. However, when signals are transmitted through the human body, signal loss may occur due to human characteristics. Especially, communication quality analysis is needed because communication quality are affected by ground plane and human body characteristics. Therefore, human body channel characteristics must be analyzed to apply HBC to the optimal application. HBC uses the human body, which is composed of a lossy dielectric material, as the transmission medium; therefore, the data signal from wearable devices can be transmitted without any wireless or wired connection. In comparison with general wireless communication, the HBC consumes less power while supporting a high data rate of over 1 Mbps because it uses a low-frequency band under 120 MHz [2 - 4]. Some previous studies [5 - 7] have investigated the transmission characteristics of the human body channel while others [8 - 10] have reported on the development of transmitter and receiver chips. The correlation-based transceiver attenuates signals that correlate with unexpected signals [8], and adaptive frequency hopping(AFH) is a modulation scheme used to improve resistance to in-band interferences by excluding the corrupted frequencies from the hop set [9]. The IEEE 802.15.6 BAN standard has adopted the

frequency selective digital transmission(FSDT) as the modulation scheme for HBC [11]. As the FSDT scheme uses a baseband signal without RF/IF components, it has low power consumption and can simplify analog circuits. In FSDT, data composed of 4 bits is transformed into a Walsh code of 16 chips, and then the transformed code is spread in the frequency domain using the frequency selective spreader. A data is spread in a 21 MHz center frequency region with a 5.25 MHz bandwidth using a frequency selective spreading code.

In HBC, the human body functions as a channel for data signal transmission. The human body, however, also functions as an antenna. This is due to the fact that the tissues of the human body have a high dielectric constant in the frequency band used for the signal transmission; accordingly, the wavelength inside the human body becomes comparable to the physical size of the human body [1 - 2]. An HBC user is surrounded by various electronic devices while those devices radiate electromagnetic waves. As the human body functions as an antenna, it receives the radiated electromagnetic waves; consequently, an interference signal is generated in the human body channel. When an HBC receiver receives a data signal transmitted through the human body channel, the generated interference signal causes signal interference at the HBC receiver. Such signal interferences have been investigated in several studies [5], [8 - 9], [13 - 15]. Because the human body is influenced by various physical characteristics and ground plane, communication performance analysis is needed. In order to apply optimal HBC to wearable devices, it is necessary to analyze the characteristics and parameters of various human channels and analyze the performance of HBC according to human body characteristics. In [5] and [8 - 9], the effects of signal interference on the bit error rate(BER) performance were analyzed with respect to different modulation schemes, such as AFH and input clamping. Those studies, however, did not consider the modulation scheme defined in the IEEE 802.15.6 BAN standard. In [13 - 14], the signal interference was analyzed with respect to the modulation scheme of the IEEE 802.15.6 BAN

standard. In those studies, a BER degradation model was proposed to predict the BER performance when co-channel interference occurs. In [15], an interference signal model was derived after measuring the interference signals in general electromagnetic environments. The interference signal model was then used to predict the BER performance of an HBC receiver supporting the IEEE 802.15.6 BAN standard. Those studies, however, did not consider the different aspects of receiver performance, such as synchronization accuracy and inter-symbol interference(ISI), during the BER performance analysis. The BER performance is strongly affected by the receiver performance. If the HBC receiver has decreased synchronization accuracy or if there is considerable ISI in the filter used for the HBC receiver, the BER performance is degraded further; therefore, the receiver's performance should be considered in the BER performance analysis. The BER performance can then be predicted more practically under an interference environment. In addition, although HBC can provide intuitive and simple service, it is very difficult to apply to a multimedia data transmission system due to limitation of data rate and contact for data transmission. Therefore, in this thesis, an application system was proposed that can overcome these disadvantages of HBC.

II. Performance evaluation of human body communication using FSDT

A. Analysis of human body channel characteristics

To evaluate the reception performance of the background interference signal of the HBC transceiver using the FSDT, it is necessary to take into consideration the characteristics of the human body channel. In HBC, the human body functions as a channel for data signal transmission. The human body also functions as an antenna. Because HBC is transmitted through the skin and deeper tissues of the human body, it is greatly influenced by various parameters of the human body and the surrounding environment [16]. This is due to the fact that the tissue of the human body has a high dielectric constant in the frequency band used for signal transmission. The wavelength of this frequency band is similar to the physical size of the human body. Since the HBC is affected by various physical characteristics of the human body and the ground plane, it is necessary to analyze the characteristics of the received signal according to the human body channel characteristics.

To evaluate the reception performance of HBC transceiver using FSDT considering the characteristics of the human channel, the signal attenuation characteristics and time delay characteristics of the human channel were analyzed. Human body channel characteristics was analyzed through impulse response characteristics. The signal attenuation characteristics of human body according to the frequency change can be analyzed through the impulse response characteristic. The time delay characteristics of the human body channel also measured for synchronization of the transmission and reception signals. Time delay characteristics is important for analysis of the BER performance of the HBC using FSDT. The time delay characteristics of body channel was analyzed by calculating the power delay profile(PDP), mean delay and root-mean-square(RMS) delay for the impulse response. For confirming correlation of the human body characteristics and signal loss

characteristics for the HBC, impulse response and body characteristics of 120 subjects were measured. Table 2.1 shows informations on subjects of 120 experimental groups. Correlation coefficient was analyzed with body characteristics and signal transmission direction and impulse response of body channel.

Table 2.1 Subjects for human body channel analysis

Items	Specification
Gender	male
The number of subjects	120
Age	20 ~ 30
Transmission direction	chest → wrist (patch to watch), wrist → chest (watch to patch)
Body characteristics	weight, muscle, fat mass, total body water

1. Measurement setup for analysis of body channel characteristics

In this study, a watch and patch transmitter and receiver were fabricated to analyze the channel for wearable devices attached to various positions of the human body.

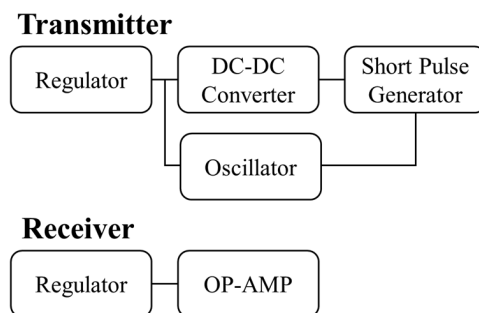


Figure 2.1 Diagram of channel model transmitter and receiver

Figure 2.1 shows the transmitter and receiver diagrams for measuring the impulse response characteristics of the conductive channel. Since the body channel is a conductive medium but has a high resistance value, the output signal of the transmitter must be amplified to transmit the impulse signal through the human body. The transmitter uses an oscillator to generate a signal with a frequency of 1.5 MHz and a period of 11 ns. In the regulator, 3.3V is output to operate the oscillator. The voltage for operating the short pulse was converted from 3.3V to 5V output from the regulator through a DC-DC converter. The receiver amplifies the transmitted pulse signal through the conductive channel by about 18 dB. The patch type module was designed to attach three electrodes in consideration of the device placed in the chest. Watch type module was designed considering smart watch or smart band. Figure 2.2 shows a patch-type and a watch-type transmitter for measuring the impulse response characteristics of a body channel, and Figure 2.3 shows a patch-type and a watch-type receiver.

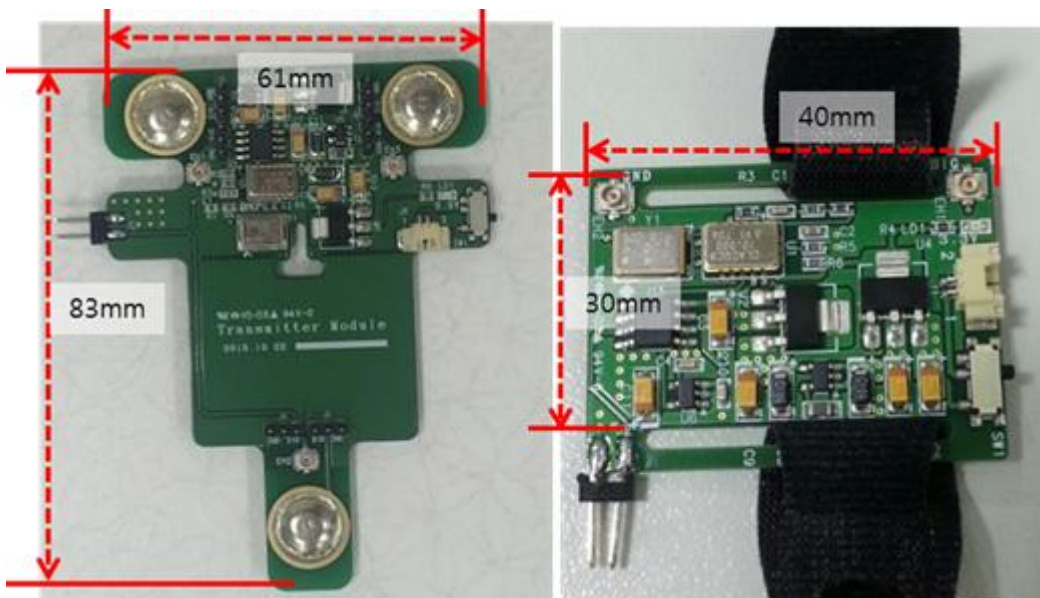


Figure 2.2 (left) Patch type, (right) watch type channel modeling transmitter

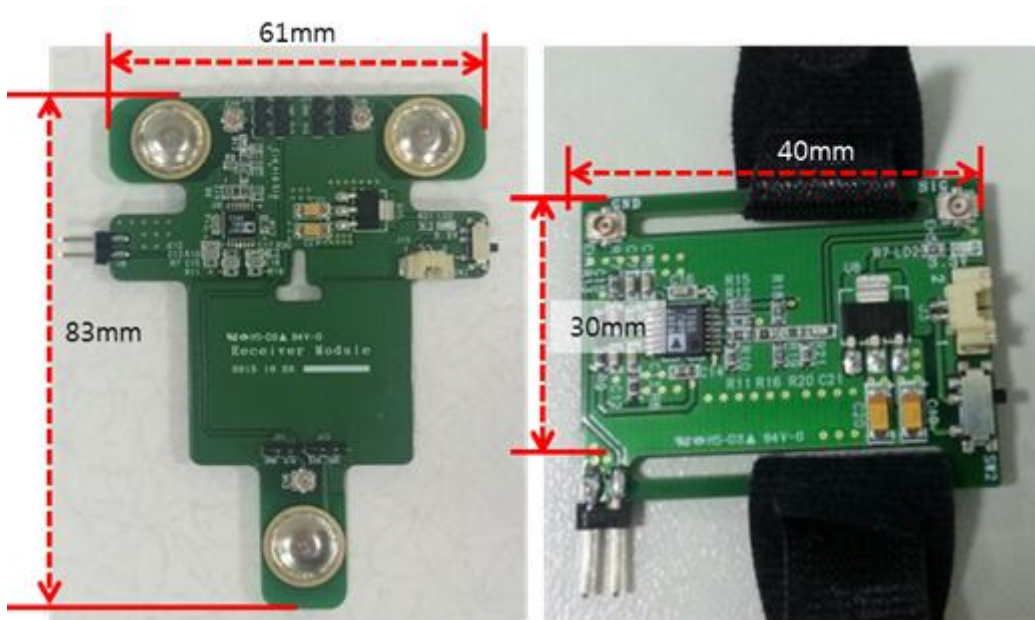


Figure 2.3 (left) Patch type, (right) watch type channel modeling receiver

Body weight, body fat mass, muscle mass, and total body water were measured in 120 male using an In-body meter(InBody770 from InBody Corp.). The signal loss characteristics of the HBC module were analyzed according to the body characteristics. Figure 2.4 shows the body measurement setup.

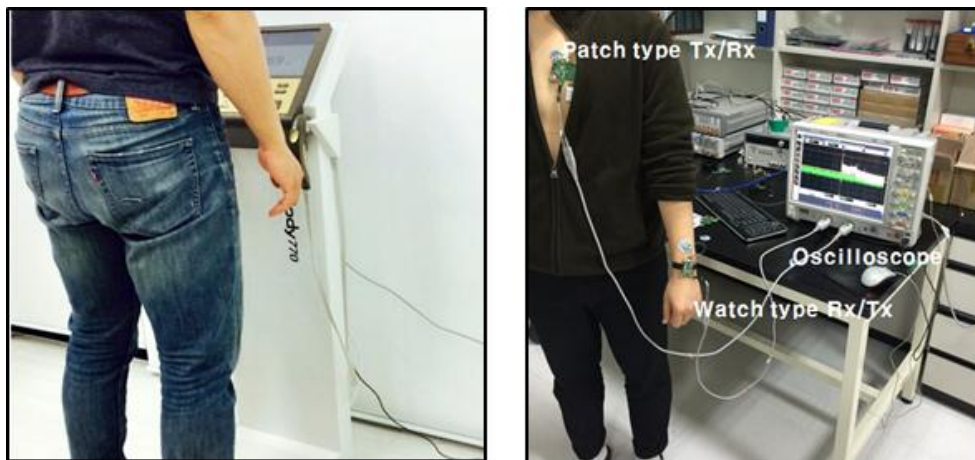


Figure 2.4 (left) Measurement setup of body characteristics, (right) measurement setup for impulse response characteristics

HBC signal characteristics were measured using Foam electrodes(31118733 form Kendal), an oscilloscope(MSO9104A from Agilent) and an active probe(1131A probe from Agilent). Figure 2.5 shows the impulse response characteristic measurement setup. The subjects were measured in standing position and the position and the shape were the same. The patch type transceiver was attached 3cm from the nipple area of the left chest. The watch type transceiver was placed on the wrist and the electrode was attached about 2cm from the module to keep the transmission and reception distance to about 45cm.

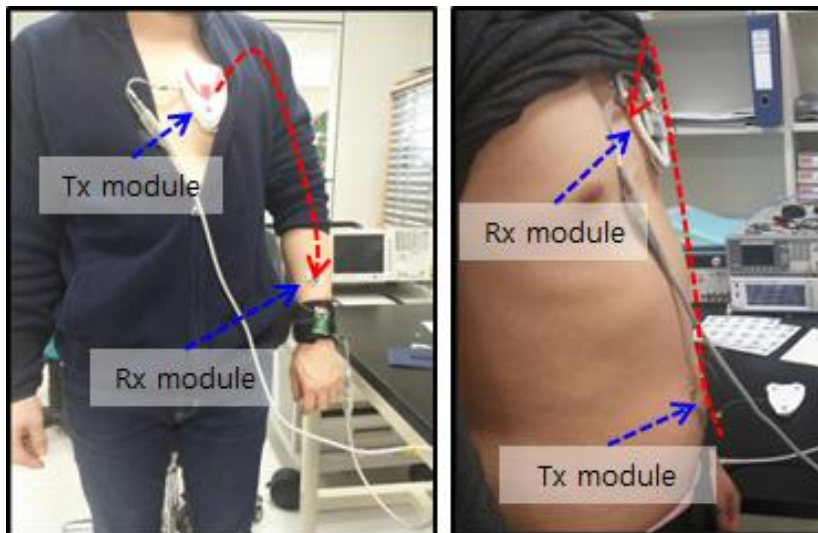
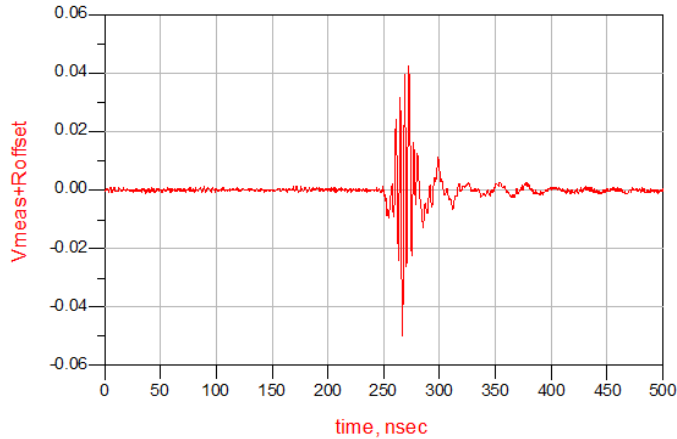


Figure 2.5 Measurement setup for impulse response characteristics (left) patch to watch, (right) watch to patch

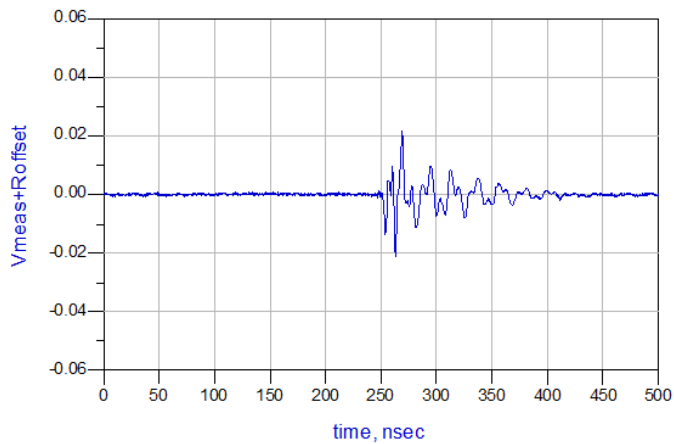
To analyze the time delay characteristics of the body channel, the power delay profile(PDP), mean delay, and root mean square(RMS) delay were calculated. In order to form a ground plane similar to the HBC conditions applied to mobile devices, the body channel characteristics were measured by blocking the DC coupling by the measuring device using balun on the measurement probe.

2. Measurement results of body channel characteristics

A) Signal loss characteristics



(a)



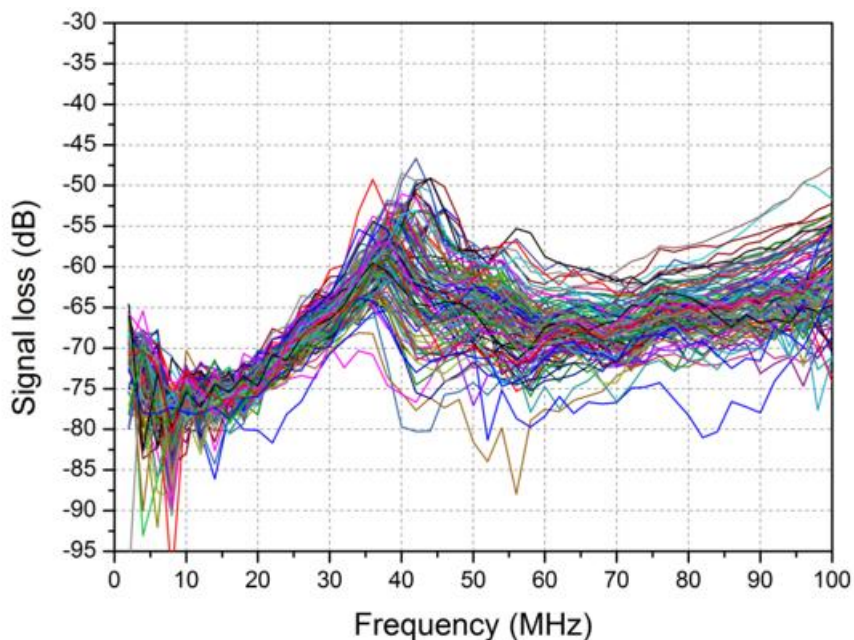
(b)

Figure 2.6 (a) Output signal of patch type receiver, (b) output signal of watch type receiver

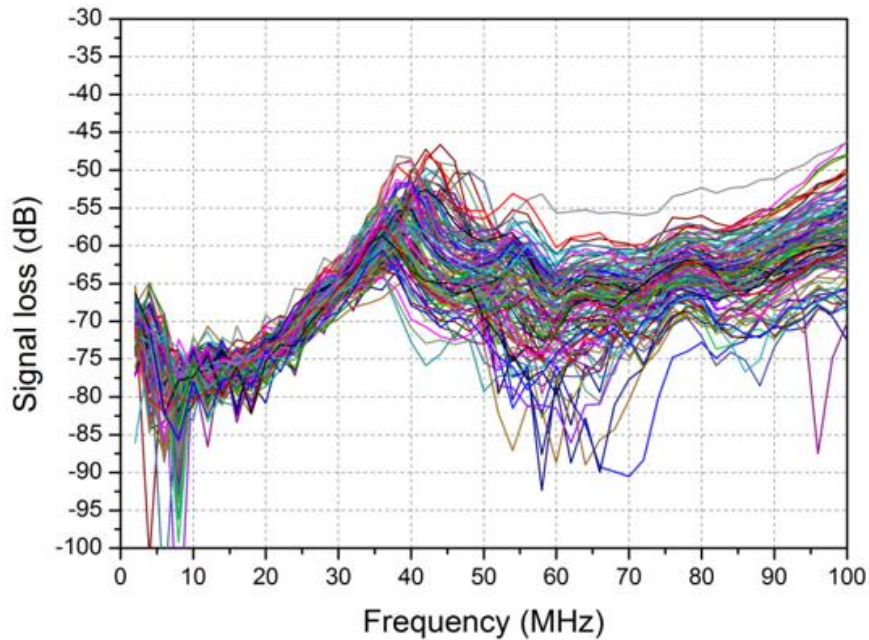
Figure 2.6 (a) shows the patch type transmitter and watch type receiver, and (b) shows the received signal output of the watch type transmitter and

the patch type receiver. The horizontal axis is the time axis from 0 to 500 ns, and the vertical axis is the signal strength from -0.06 to 0.06. The time domain received signal was amplified 18 dB through the AMP of the receiver. The magnitude of the received signal was measured at 93 mV(a) and 43 mV(b).

To obtain the impulse response characteristics, the signal loss values of 120 subjects are summarized by the histogram according to the directions of transmission and reception of the respective impulse signals. Then, using the low pass filter of 100 MHz through Matlab, the data of the subjects are summarized as the following graph. The average signal loss of the human channel was -65 dB above the 60 MHz band when transmitted from the chest to the wrist. The average signal loss when transmitting from the wrist to the chest was -64 dB above the 60 MHz band.



(a)



(b)

Figure 2.7 Signal loss (a) patch to watch, (b) watch to patch

Figure 2.7 shows the signal loss through the body channel modeling device according to the transmission direction in the frequency band from 1 MHz to 100 MHz. The signal loss exhibited capacitive coupling characteristics in the low frequency band and resonance occurred at around 40 MHz. In the band below 40 MHz, the characteristic that the signal loss decreases with increasing frequency is similar to the characteristic that the impedance decreases with decreasing signal loss according to increasing frequency of the capacitor. Therefore, it can be seen that capacitive coupling characteristic is in the band below 40 MHz. Because the change of the signal loss from the low frequency band to the 40 MHz is large, it is not suitable as a frequency band for HBC. The frequency band over 60 MHz is more flat than other frequency bands, so it is suitable as a frequency band for HBC.

B) Time delay characteristics

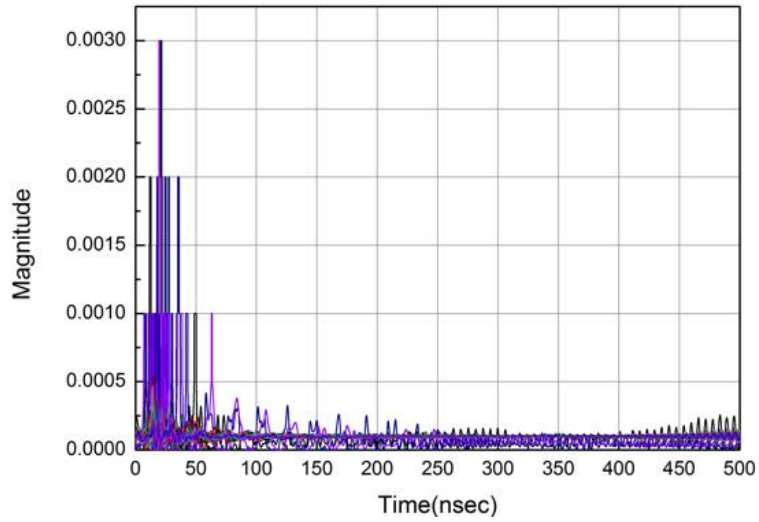
To analyze the time delay characteristics of the body channel, we analyzed PDP obtained by using the impulse response of the body channel. The PDP was calculated as the square root of the second moment of time and power. In a typical wireless channel, the random signal loss and delay of each path change with time. The impulse response is represented by a time function t and a delay τ : $h(t, \tau)$. Each subject's signal loss and PDP were used to obtain three-channel parameters: (1) average signal loss; (2) Mean Delay; and (3) RMS Delay.

$$P(\tau) = |h(\tau)|^2 \quad (1)$$

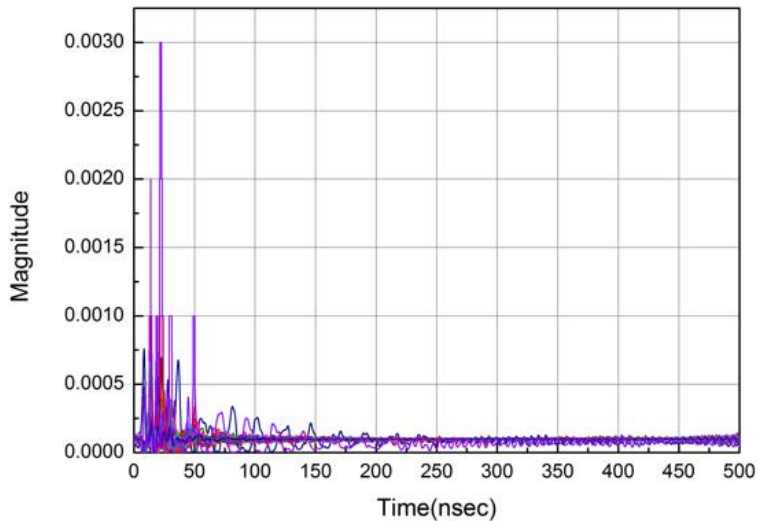
$$\tau_{Mean} = \frac{\sum_k P(\tau_k) \tau_k}{\sum_k P(\tau_k)} \quad (2)$$

$$\sigma_\gamma = \sqrt{\tau_{Mean}^2 - \tau_{Min}^2} \quad (4)$$

The average signal loss is calculated by averaging the signal loss magnitude of all frequencies. The mean delay, which means the average value of the delay, can be calculated by multiplying the power value by the PDP and dividing by the total power value. The RMS Delay indicates the degree of spread of the power value and the time value of the Mean Delay value. Figure 2.9 shows the time delay characteristics of 120 subjects according to the direction of signal transmission and reception through the PDP.



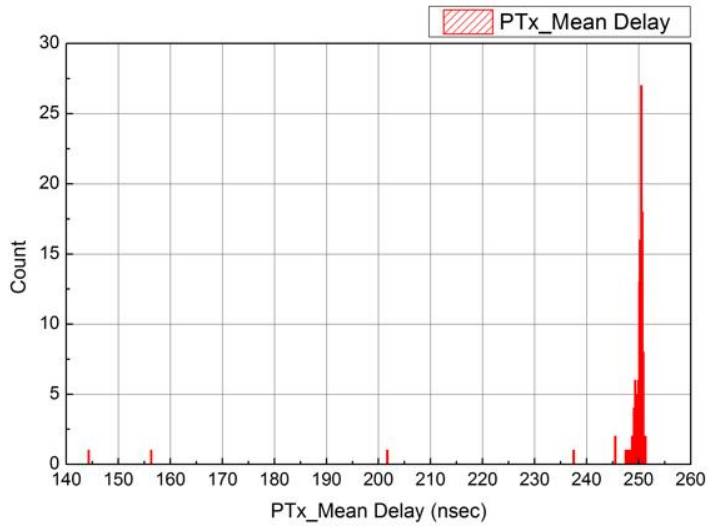
(a)



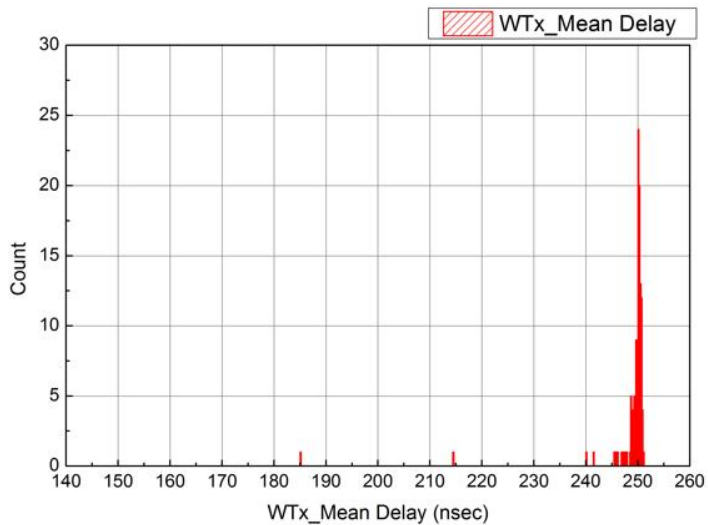
(b)

Figure 2.8 Power delay profile (a) patch to watch, (b) watch to patch

Figure 2.8 shows the average time delay characteristics according to the direction of transmission and reception. The average time delay of the transmission from the chest to the wrist was 250.4, and the average delay of 250.225 was transmitted from the wrist to the chest.



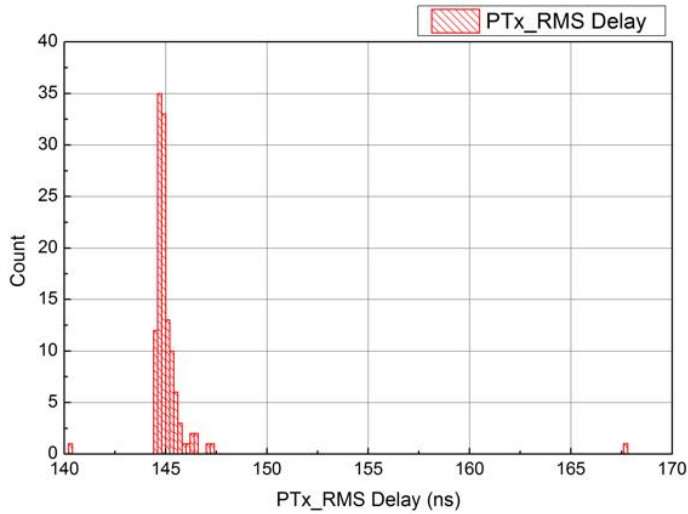
(a)



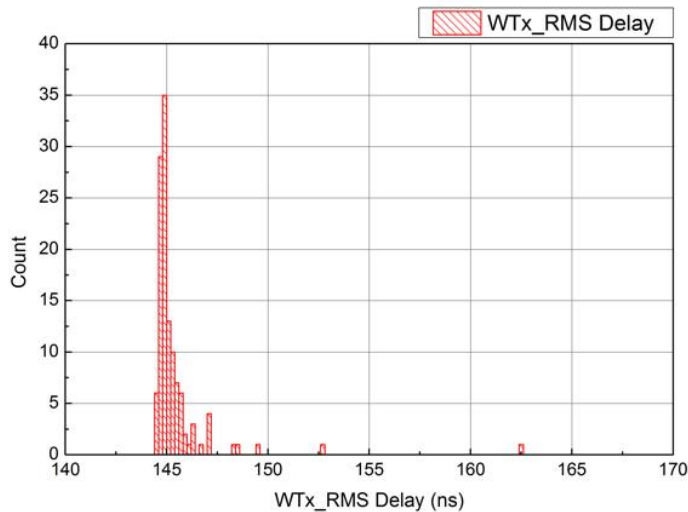
(b)

Figure 2.9 Mean delay (a) patch to watch, (b) watch to patch

Figure 2.9 shows the RMS delay characteristics according to the direction of transmission and reception. The RMS delay is 145.31 when transmitted from the chest to the wrist, and the average is 145.37 when transmitted from the wrist to the chest.



(a)



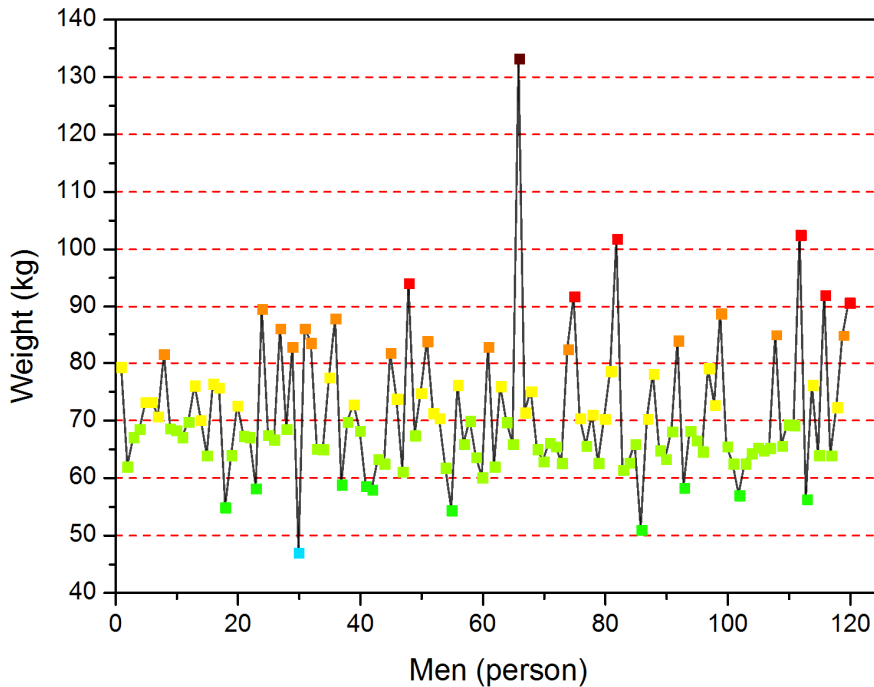
(b)

Figure 2.10 RMS delay (a) patch to watch, (b) watch to patch

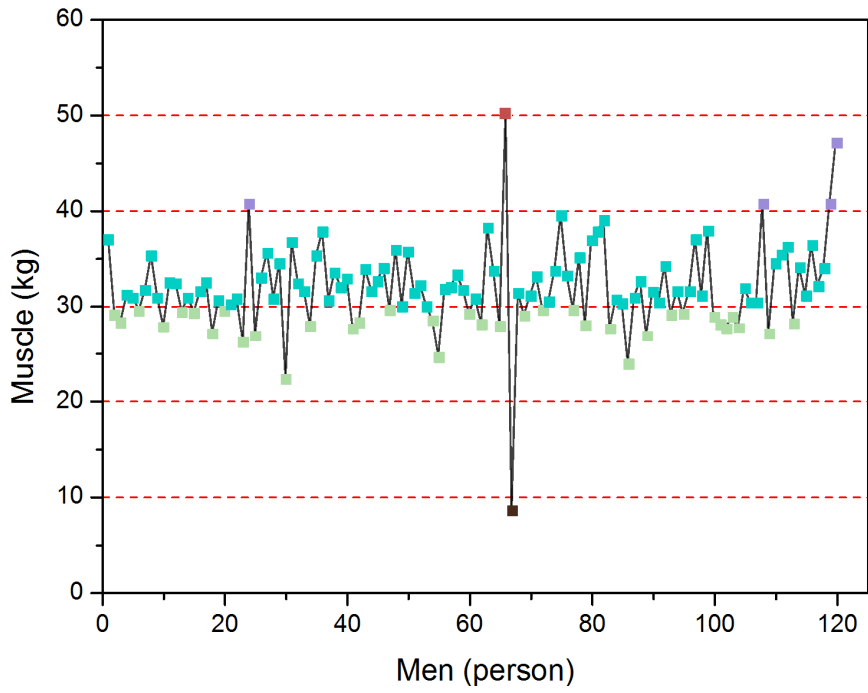
The results of these measurements show that the design of receiver for HBC device should be designed considering the average time delay characteristics for timing synchronization. This result is also a characteristic of the human body channel to be considered for synchronization of the transmission and reception signals for the BER performance analysis of the HBC transceiver using FSDT.

3. Correlation characteristics

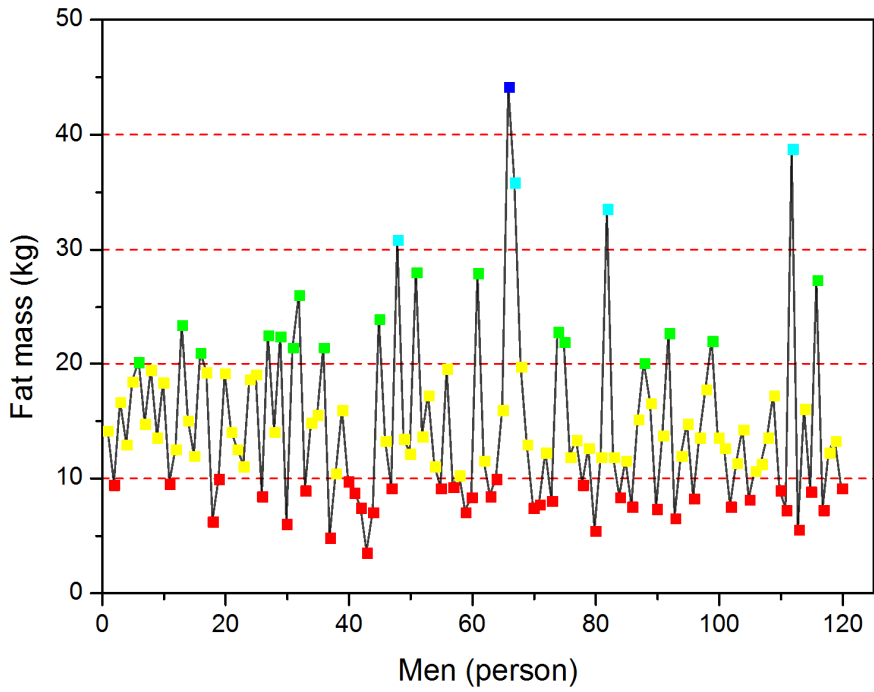
Since the characteristics of the human channel are expected to be influenced by the body characteristics, the correlation between the measured body channel characteristics and the body characteristics of 120 subjects was analyzed. To analyze the body channel characteristics according to body characteristics, the signal loss and time delay were measured in the two directions of transmission from the chest to the wrist and from the wrist to the chest. The correlation was analyzed in eight conditions including body weight, body fat mass, muscle mass, and total body water, which are body characteristics for the experimental group. Figure 2.11 shows the measurement data of measured human body composition conditions for 120 adult male subjects.



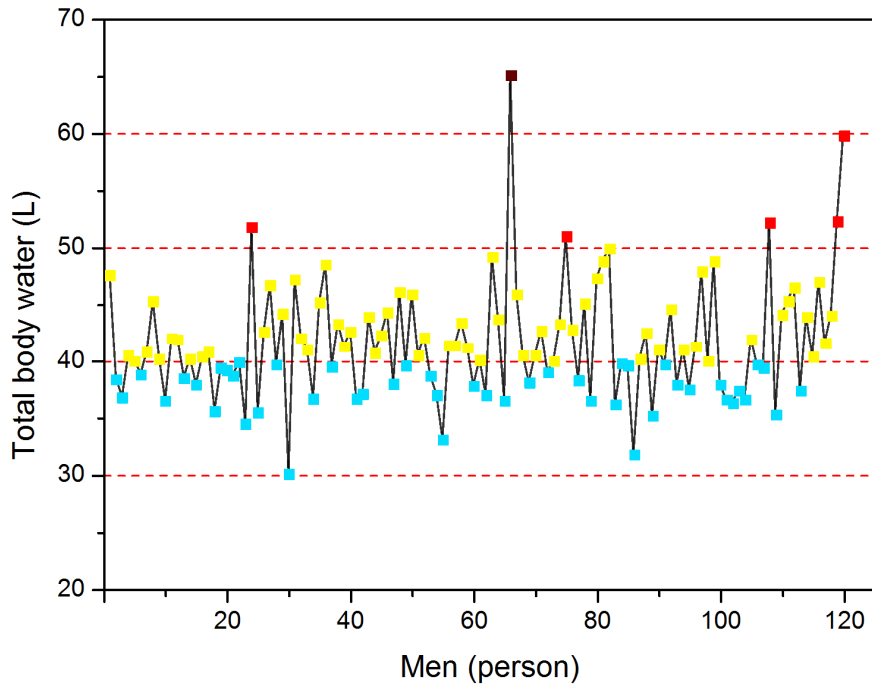
(a)



(b)



(c)



(d)

Figure 2.11 (a) Weight, (b) muscle, (c) fat mass, (d) total body water analysis graph for the experimental group

Pearson correlation coefficient was used for correlation analysis between human body characteristics and signal loss and time delay characteristics. Equation (4) to find the correlation ρ_{SC} between body characteristics and channel characteristics is as follows

$$\rho_{SC} = \frac{E\{(S - \mu_S)(C - \mu_C)\}}{\sigma_S \sigma_C} \quad (4)$$

S is the value of signal loss and C is the value of body characteristic. σ_S is the standard deviation of the signal loss and σ_C is the standard deviation of the body characteristic. μ_S is the mean value of the signal loss and μ_C is the mean value of each body characteristics. E represents the expected value. The correlation coefficient is represented by a numerical value of $0 < \rho \leq 1$

and can be classified as follows.

- $\pm 0.1 < \rho \leq \pm 0.3$ Weak linear relationship
- $\pm 0.3 < \rho \leq \pm 0.7$ Definite linear relationship
- $\pm 0.7 < \rho \leq \pm 1$, a strong linear relationship

A) Correlation between signal loss and body characteristics

Correlation coefficients were calculated to analyze the correlation of each condition through the signal loss over 40 MHz band. Since the frequency band suitable for the HBC was confirmed through analyzing the characteristics of the receiving channel of the human body channel, the average value of the signal loss for the correlation analysis was the band of 40 MHz or more. The average and standard deviation of the signal loss according to the variation of the human body characteristics are summarized to obtain the correlation between the human characteristics and the signal loss over 40 MHz band. Table 2.2, 2.3, 2.4, and 2.5 show the mean and standard deviation of the signal loss for each human body according to changes in signal transmission direction and human body characteristics.

Table 2.2 Average and standard deviation of signal loss by weight of experimental group

Weight (kg)	Patch → Watch		Watch → Patch	
	Average (μ_P)	Standard deviation (σ_P)	Average (μ_W)	Standard deviation (σ_W)
80 ~ over	-67.3 dB	3.37	-65.7 dB	4.65
70 ~ 80	-65.4 dB	2.76	-64.9 dB	3.48
60 ~ 70	-64.8 dB	2.31	-63.5 dB	2.66
under ~ 60	-62.6 dB	2.75	-60.7 dB	2.75

Table 2.3 Average and standard deviation of signal loss by muscle of experimental group

Muscle (kg)	Patch → Watch		Watch → Patch	
	Average (μ_P)	Standard deviation (σ_P)	Average (μ_W)	Standard deviation (σ_W)
40 ~ over	-68.1 dB	5.06	-65.9 dB	6.19
30 ~ 40	-65.5 dB	2.81	-64.3 dB	3.42
20 ~ 30	-64.4 dB	2.57	-62.9 dB	3.26
under ~ 20	-65.8 dB	-	-67.0 dB	-

Table 2.4 Average and standard deviation of signal loss by fat mass of experimental group

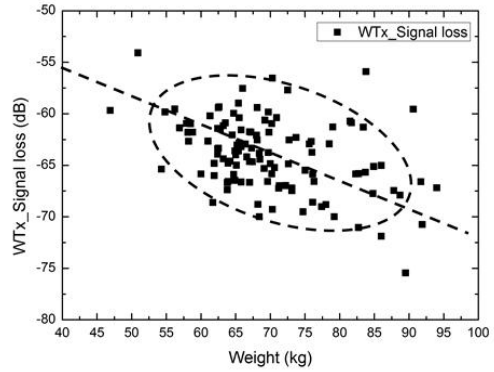
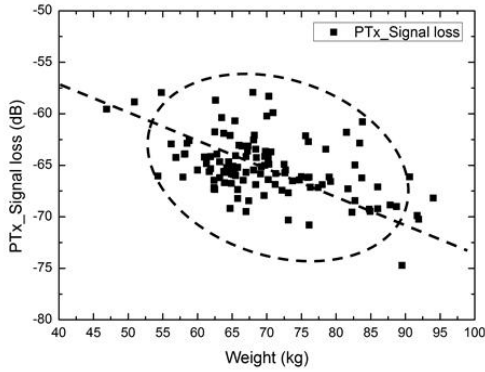
Fat mass (kg)	Patch → Watch		Watch → Patch	
	Average (μ_P)	Standard deviation (σ_P)	Average (μ_W)	Standard deviation (σ_W)
30 ~ over	-66.3 dB	3.23	-65.4 dB	3.66
20 ~ 30	-67.0 dB	2.82	-65.9 dB	4.06
10 ~ 20	-65.2 dB	2.87	-64.3 dB	3.52
under ~ 10	-64.5 dB	2.76	-62.4 dB	2.78

Table 2.5 Average and standard deviation of signal loss by total body water of experimental group

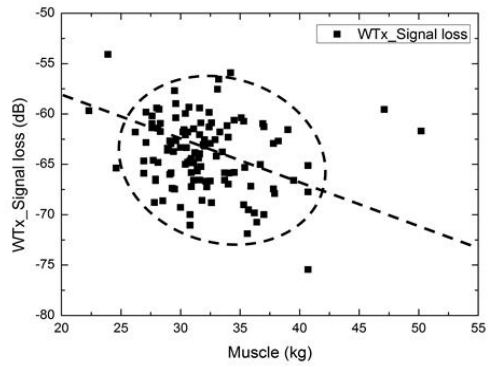
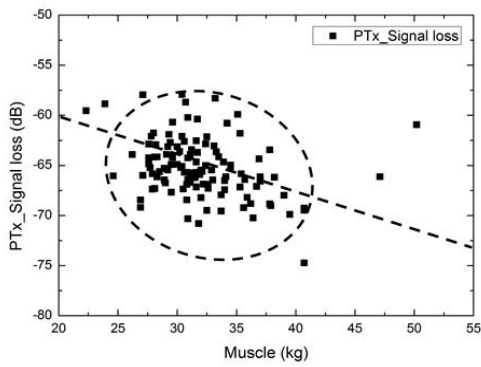
Total body water (L)	Patch → Watch		Watch → Patch	
	Average (μ_P)	Standard deviation (σ_P)	Average (μ_W)	Standard deviation (σ_W)
60 ~ over	-60.9 dB	-	-61.7 dB	-
50 ~ 60	-69.9 dB	3.08	-66.9 dB	5.72
40 ~ 50	-65.7 dB	2.63	-64.4 dB	3.45
30 ~ 40	-64.1 dB	2.62	-63.1 dB	3.26

Figure 2.12 shows the distribution of correlation coefficients according to each human body characteristic. The correlation coefficient of the signal loss

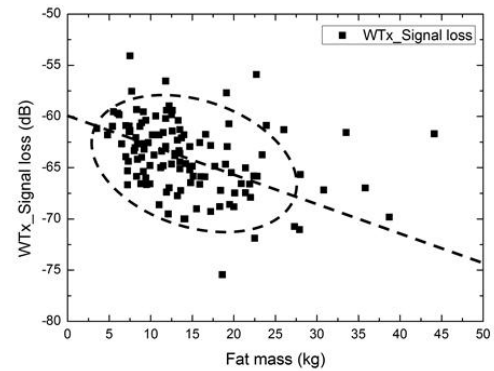
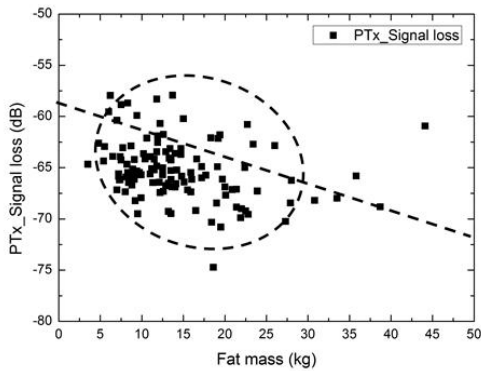
with respect to the body characteristic shows the negative results as a whole.



(a)



(b)



(c)

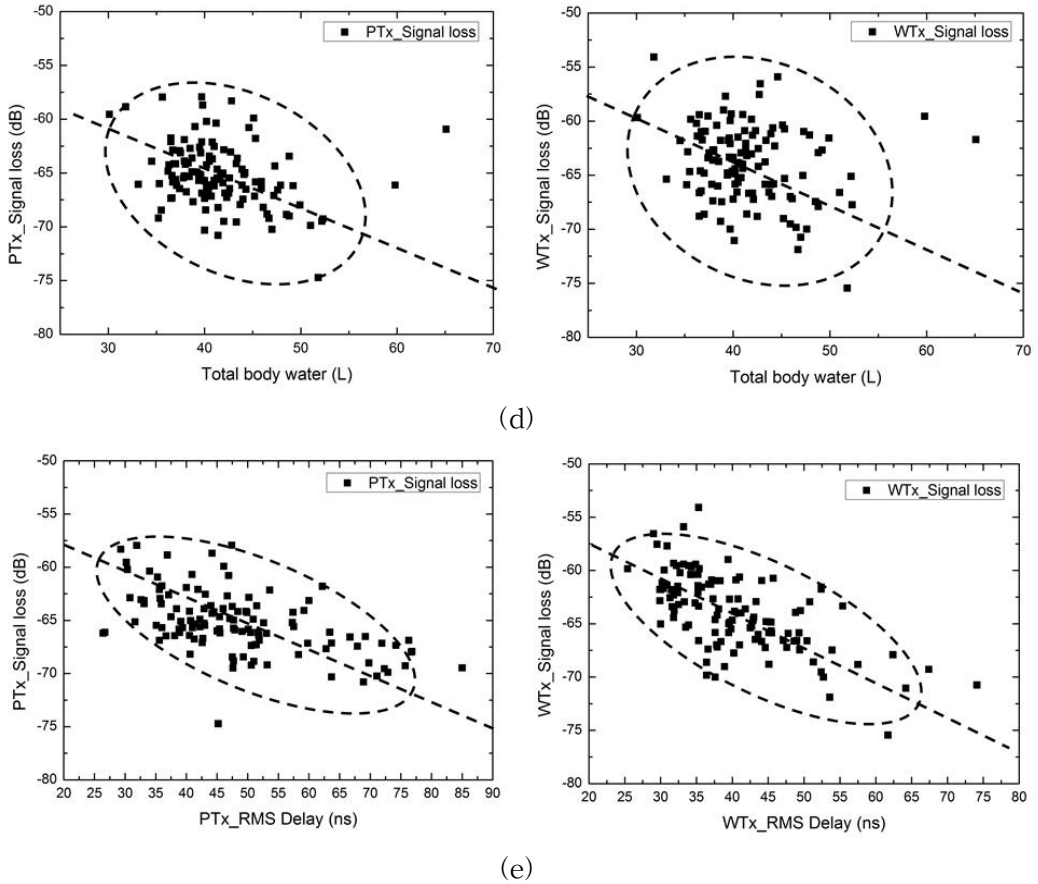


Figure 2.12 Correlation scatter diagram of signal loss according to body characteristics (a) weight, (b) muscle, (c) fat mass, (d) total body water, (e) RMS delay

Table 2.6 shows the correlation coefficients of signal loss and time delay according to differences in human body characteristics.

Table 2.6 Correlation coefficient of signal loss according to body characteristics

Communication direction	Weight	Muscle	Fat mass	Total body water	RMS delay
Patch → Watch	-0.354	-0.263	-0.285	-0.300	-0.535
Watch → Patch	-0.320	-0.141	-0.348	-0.196	-0.628

The correlation coefficient of human body characteristics with signal loss shows a generally weak linear relationship value of -0.3 for each human body characteristic. In particular, the muscle mass has the least correlation coefficient with respect to the change of the signal loss, so that the muscle mass has the least effect on the human body channel signal loss compared to the body fat mass. The weight of the human body has a relatively large correlation. Because the volume of the body increases with the increase of the body characteristics, the length of the human channel becomes longer. The total body water of the human body also did not show a relatively large correlation. The low correlation between the signal loss characteristic and the total body water is due to the fact that the total body water does not greatly affect the volume of the human body. The correlation coefficient between time delay and signal loss is relatively higher than the correlation coefficient for body characteristics. As a result, the signal loss increases as the time delay increases. The reason why the correlation between the signal loss and the time delay characteristic is relatively high is that as the human body volume increases, the length of the human body becomes longer, which leads to a larger signal loss and a larger time delay.

B) Correlation between time delay and body characteristics

Table 2.7, 2.8, 2.9, and 2.10 show the mean and standard deviation of the signal loss for each human body according to changes in signal transmission direction and human body characteristics.

Table 2.7 Average and standard deviation of time delay by weight of experimental group

Weight (kg)	Patch → Watch		Watch → Patch	
	Average (μ_P)	Standard deviation (σ_P)	Average (μ_W)	Standard deviation (σ_W)
80 ~ over	55.6 ns	15.22	45.0 ns	12.12
70 ~ 80	52.3 ns	12.72	42.9 ns	8.94
60 ~ 70	45.4 ns	10.19	38.3 ns	6.83
under ~ 60	40.9 ns	9.17	36.3 ns	4.55

Table 2.8 Average and standard deviation of time delay by muscle of experimental group

Muscle (kg)	Patch → Watch		Watch → Patch	
	Average (μ_P)	Standard deviation (σ_P)	Average (μ_W)	Standard deviation (σ_W)
40 ~ over	53.6 ns	25.51	39.7 ns	12.85
30 ~ 40	49.6 ns	13.05	41.1 ns	9.53
20 ~ 30	45.7 ns	8.70	39.0 ns	6.73
under ~ 20	45.4 ns	-	41 ns	-

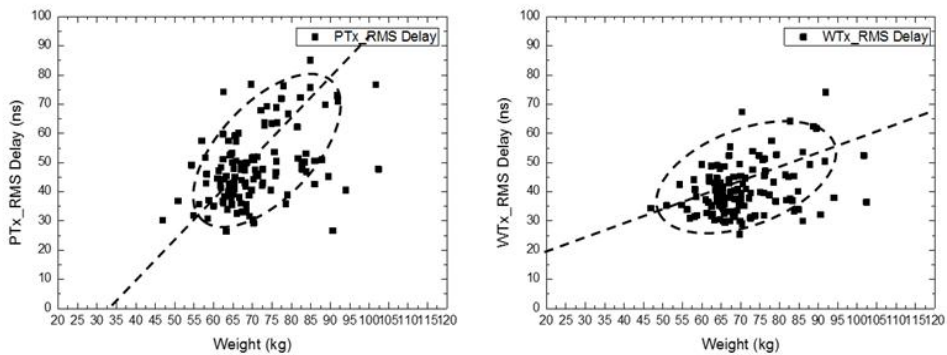
Table 2.9 Average and standard deviation of time delay by fat mass of experimental group

Fat mass (kg)	Patch → Watch		Watch → Patch	
	Average (μ_P)	Standard deviation (σ_P)	Average (μ_W)	Standard deviation (σ_W)
30 ~ over	50.9 ns	14.35	47.3 ns	5.43
20 ~ 30	48.8 ns	11.22	40.3 ns	8.85
10 ~ 20	47.9 ns	12.32	40.9 ns	8.77
under ~ 10	49.2 ns	13.74	38.9 ns	9.15

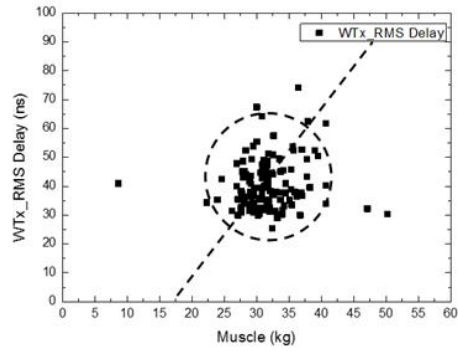
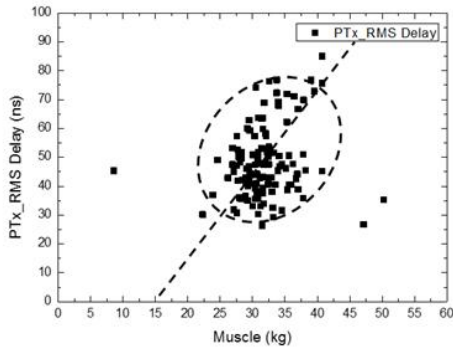
Table 2.10 Average and standard deviation of time delay by total body water of experimental group

Total body water (L)	Patch → Watch		Watch → Patch	
	Average (μ_P)	Standard deviation (σ_P)	Average (μ_W)	Standard deviation (σ_W)
60 ~ over	66.7	-	52.7	-
50 ~ 60	50.1	13.35	47.6	5.74
40 ~ 50	46.8	10.52	40.7	8.84
30 ~ 40	50.3	14.79	39.1	8.79

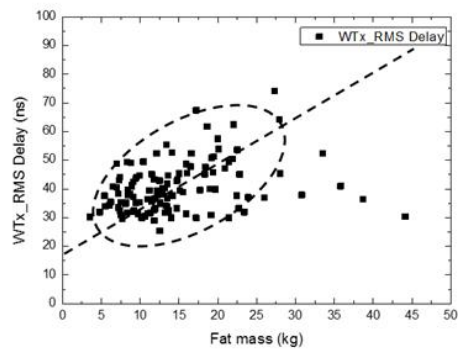
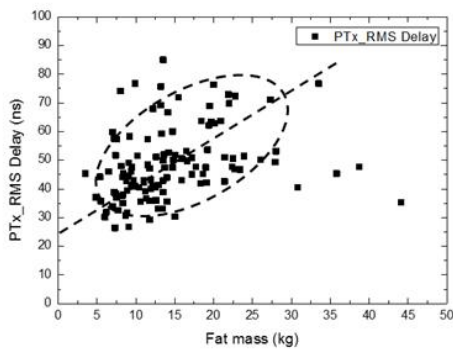
Figure 2.13 shows the distribution of correlation coefficients according to each human body characteristic. A 100 MHz low pass filter was used for the impulse response data of 120 subjects in order to improve the accuracy of correlation analysis between time delay characteristics and human body characteristics. Correlation coefficients between time delay characteristics and body characteristics show positive results as opposed to correlation coefficients between signal loss and body characteristics. These results show that the time delay increases with increasing body characteristics of the human body. This correlation shows a similar characteristic to the correlation between signal loss and body characteristics. It can be seen that the time delay characteristic also increases as the volume of the human body increases.



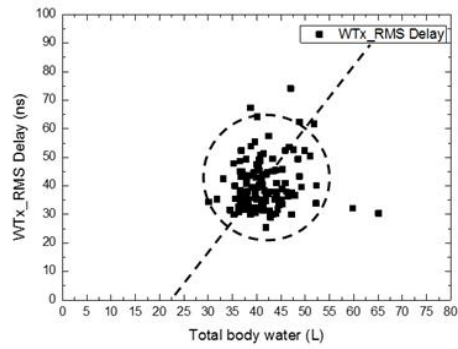
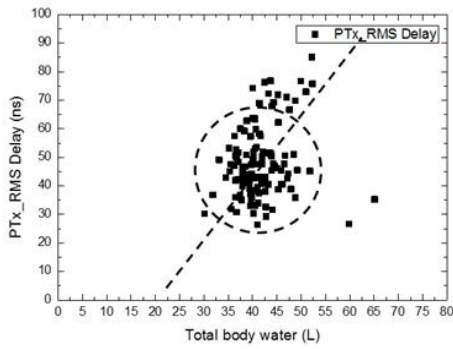
(a)



(b)



(c)



(d)

Figure 2.13 Correlation scatter diagram of time delay according to body characteristics (a) weight, (b) muscle, (c) fat mass, (d) total body water

Table 2.11 shows the correlation coefficients of signal loss and time delay according to differences in human body characteristics.

Table 2.11 Correlation coefficient of time delay according to body characteristics

Communication direction	Weight	Muscle	Fat mass	Total body water
Patch → Watch	0.316	0.200	0.296	0.209
Watch → Patch	0.256	0.099	0.306	0.110

The time delay characteristics show relatively low correlation with the body characteristics compared to the signal loss. In particular, the correlation between muscle mass and total body water is very low. This result shows that the time delay characteristic is not significantly affected by total body water content of the human body.

C) Analysis of correlation characteristics

As the body weight increases, the volume of the human body increases, and the length of the human channel increases, so that the signal loss and the time delay characteristics are increased by analyzing the correlation coefficient between the body characteristics and the body channel characteristics. The increase in weight is equivalent to the increase in fat mass and muscle. In particular, correlation coefficient analysis between fat mass and channel characteristics shows that the increase in signal loss and the increase in time delay correlated with the increase in body fat mass. This result shows that weight increases with increasing fat mass, and that the increase in signal loss and time delay characteristics are correlated. Figure 2.14 shows the correlation distribution of weight, fat mass, muscle and height. In Table 2.12, weight and fat mass are highly correlated with 0.803. This shows that as the fat mass increases, the volume of the human body increases and the length of the human body channel becomes longer. Table 2.12 shows that muscle and body weight have a very high correlation of 0.736. Figure 2.14 (b) shows the correlation distribution between body weight and muscle. As the muscle

also shows a high correlation with weight, it can be confirmed that the increase in body weight has a great correlation with the increase in muscle. However, the correlation between muscle and signal loss and time delay characteristics is relatively low compared to the correlation between body fat mass and weight. This shows that as the body weight increases, the muscle also increases, but the increase in muscle mass has a relatively low effect on the increase in the volume of the human body. This is because fat mass and muscle of the same weight have a difference in volume [17]. Fat mass and muscle are about 14 % different in volume by the same weight. Therefore, it can be seen that the body weight of two persons with the same body weight is larger than that of the fat mass. It can be seen that the signal loss and the time delay become larger as the length of the human body channel becomes longer for a person whose fat mass is larger than the muscle.

Since the correlation analysis was performed using the channel from the human body to the wrist, the body channel characteristics are changed according to the arm length of the human body. As the volume of the human body increases, the human body channel becomes longer, so that the signal loss and the time delay increase. The length of the human body channel can be changed by changing the length of the arm according to the change of the height. The analysis of correlation between weight and human body channel characteristics showed that the volume of the human body increased due to the increase in weight, and the channel characteristics were changed. Correlation coefficients were obtained to confirm the correlation between changes in height of human body and changes in weight. Table 2.12 shows that the height and weight have a correlation coefficient of 0.426. This correlation coefficient shows a relatively low correlation with the correlation between weight and fat mass or weight and muscle. The result shows that although the weight may increase when the height increases, the length of the human body channel does not increase in proportion to the height. Therefore, it can be seen that there is a weak correlation between height and body channel characteristics.

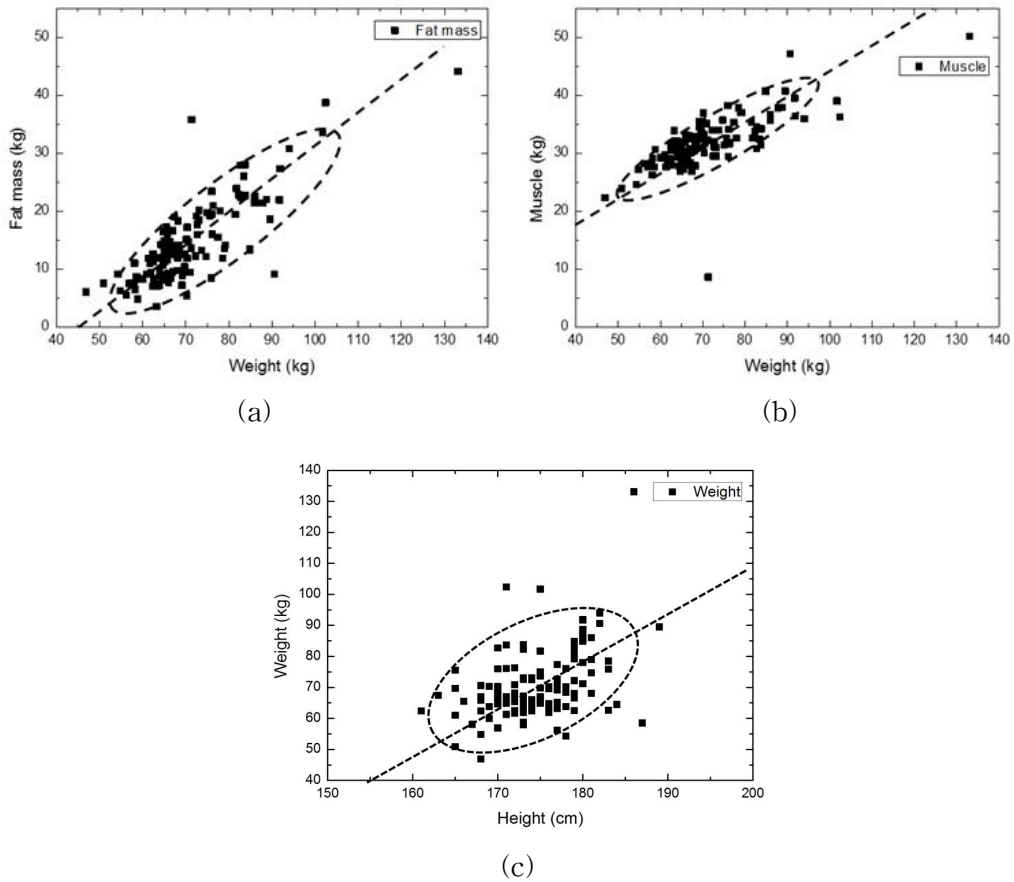


Figure 2.14 Correlation scatter diagram between body characteristics
 (a) weight-muscle, (b) weight-fat mass, (c) weight-height

Table 2.12 Correlation coefficient between body characteristics

	weight-fat mass	weight-muscle	weight-height
Correlation coefficient	0.803	0.736	0.426

B. Analysis of BER performance

This part presents the BER performance that the HBC receiver supporting FSDT experiences under an interference environment. The BER performance was investigated while considering the effects of the receiver performance on the BER performance. During the measurement, a signal attenuator was used to mimic the signal loss of the human body channel. The human body channel has a variable transmission characteristic because the channel is easy to change according to movement and posture of the human body. The signal attenuator has a constant signal loss and, consequently, the BER performance measured with the signal attenuator has improved repeatability. A data signal modulated according to the FSDT scheme was applied to the human body channel. Simultaneously, an interference signal was applied to the HBC receiver receiving the data signal through the human body channel. The BER performance was then measured at the HBC receiver.

1. Measurement setup for BER performance

In [8] and [9], the BER performance was measured when an interference signal was applied to the HBC receiver. The frequency of the interference signal was varied from 1 to 100 MHz in [8], while it corresponded to that of FM radio in [9]. In this study, the BER performance of FSDT modulation with the proposed receiver was measured under the following two interference environments:

- BER vs. interference frequency
- BER vs. SIR(out-of-band/in-band)

The FSDT scheme uses the frequency band between 8 and 22 MHz [11]; hence, the interference signal corresponds to an in-band interference signal when the generated interference signal has the frequency between 8 and 22 MHz while corresponds to an out-of-band one for other frequencies.

A) Measurement setup for BER vs. Interference frequency

The BER performance in [8] was measured versus interference frequency while the signal-to-interference ratio(SIR) was set to -2.54 dB. The BER evaluation was reproduced for FSDT modulation as applying the interference frequency from 1 to 100 MHz including in-band and out-of-band interference signals to the HBC receiver while maintaining the constant SIR of -2.54 dB.

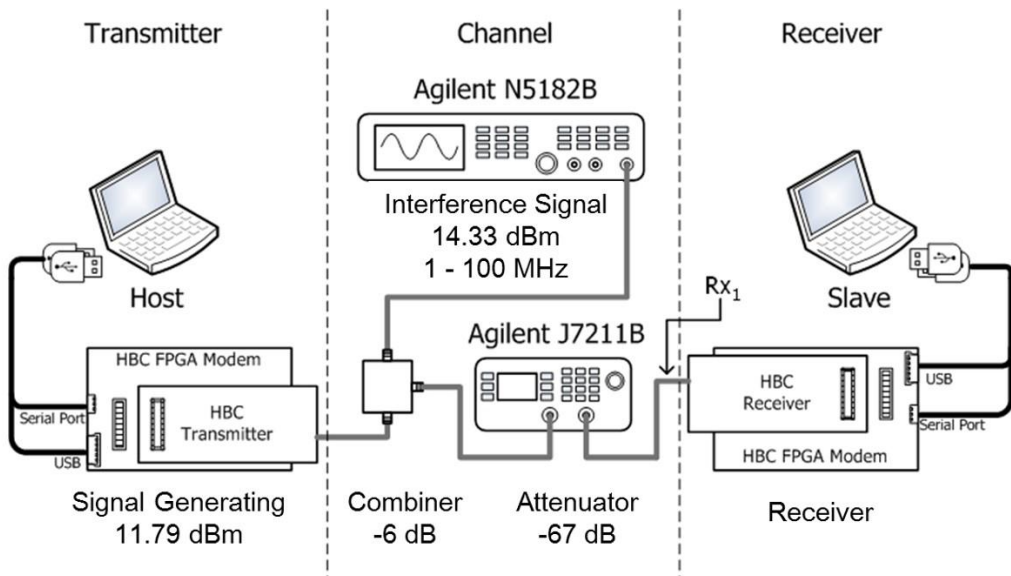
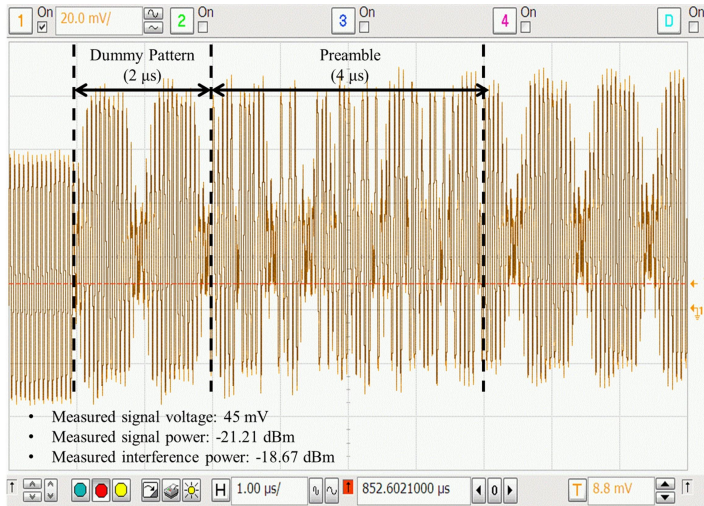


Figure 2.15 Diagram of measurement setup for BER evaluation according to the interference frequency

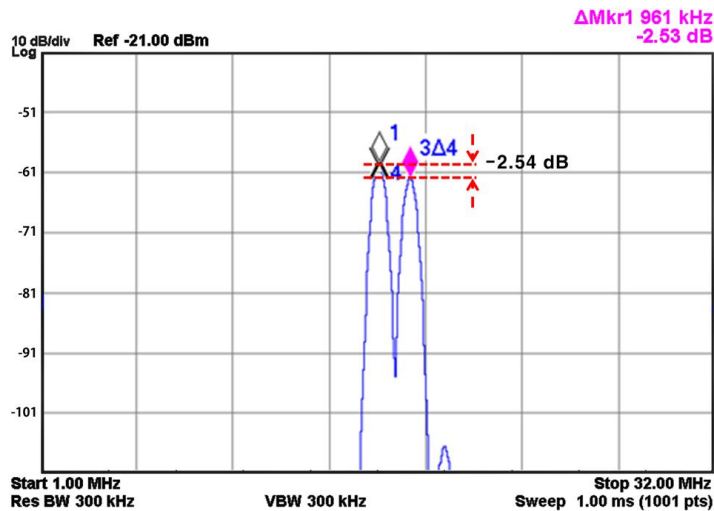
Figure 2.15 shows the measurement setup for BER evaluation according to the interference frequency. The channel loss of HBC based on the capacitive coupling mechanism is sensitive to movements, the positions of the electrodes, posture, and external ground environment [3]. To minimize the variation of the human channel, attenuator was used instead of human channel. The attenuation of the attenuator was set to -67 dB considering the signal

attenuation characteristics measured through the impulse response characteristics of the human body channel. A BER test program was used to set up the frame ratio between the master and slave, data length, number of repetitions, among others. The BER test program was installed on a laptop computer and connected to a microcontroller, which was embedded on an HBC FPGA modem. A pre-determined sequence was generated by the micro-controller. A data sequence of 1,000 bits was used as the test signal for BER evaluation, and the results were derived from the number of over 50000 data sequences of repetitive experiments to ensure reliable results. For accurate and repeatable measurements, an attenuator was used as a channel in place of the human body. The frequency step that was generated by the signal generator was set to 2.5 MHz in the 1 - 10 MHz band and 5 MHz in the 10 - 100 MHz band. For accurate performance comparison, we used not only the same SIR as presented in [8] but also the received signal with the same amplitude. To obtain the received signal level used in [8], the output signal generated by the USB dongle type transmitter needs to be decreased by -73 dB which is corresponding to the amplitude of $450 \mu\text{V}$. The attenuated signal by -73 dB was expected to be below the noise floor of the oscilloscope. To verify the amplitude of the signal by the oscillator, both the transmitting signal and interference were attenuated by -33 dB that is 40 dB larger than the signal used in the experiment. Figure 2.16(a) shows the measured signal in time domain by the oscilloscope that consists of the transmitted signal and in-band interference. The interference signal was generated by an N5182B signal generator has a frequency of 15 MHz. The attenuated signal by -33 dB from the transmitter has an amplitude of 45 mV. in this study case, the signal power and the interference power were measured as -21.21 dBm and -18.67 dBm, respectively. After confirming that the amplitude of the signal and interference, the attenuator level was increased to -73 dB, hence the signal amplitude would be $450 \mu\text{V}$. This attenuation value is set considering the signal loss value of the human channel analyzed through the impulse response characteristic of the human

channel. Figure 2.16(b) shows the measured spectrum of the signal with a power of -61.21 dBm and the interference signal with a power of -58.67 dBm that maintains SIR level of -2.54 dB. The experiments were performed through both the attenuator by increasing the frequency of interference from 1 MHz to 100 MHz.



(a)

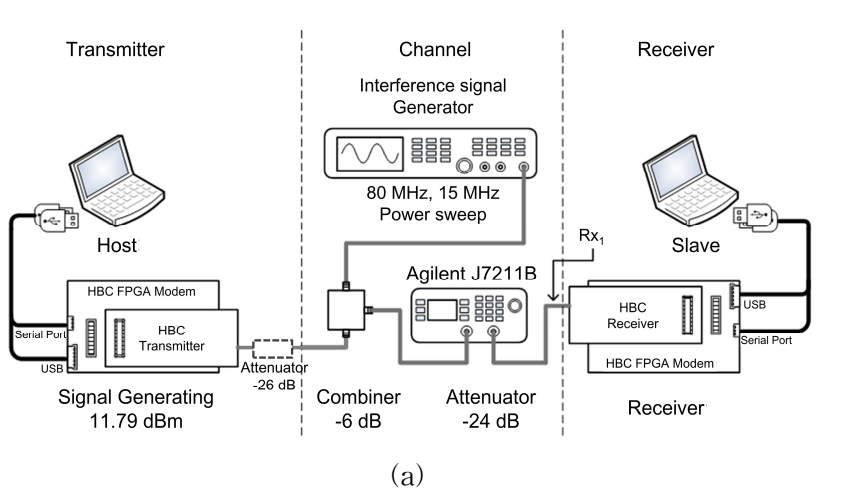


(b)

Figure 2.16 (a) Received signal at R_{x1} in Figure 2.15, (b) signal and interference power of the received signal

B) Measurement setup for BER vs. SIR

The BER performance of FSDT modulation was evaluated by increasing the power of the interference signal for the in-band and out-of-band interference signals. The largest power spectral density(PSD) was found around the 80 MHz frequency band in a previous study on interference signals induced by the human body [9]. In [9], the BER was measured according to the SIR level in the 80 MHz FM radio frequency band for the AFH modulation method. in this study, an 80 MHz continuous wave was used as the out-of-band interference signal. A continuous wave of 15 MHz, which is the nearest frequency to the modulated signal with 32 Megachips per second(Mcps), was used as the in-band interference signal for the FSDT modulation. Due to the robust characteristic of the FSDT scheme against out-of-band interference, a high interference power of 30 dB or more than the transmitted signal power was required. Due to the output power limit of the signal generator, however, an attenuator of -26 dB, which is shown as a dotted box in Figure 2.16 was inserted between the USB dongle type transmitter and the power combiner instead of increasing the interference power.



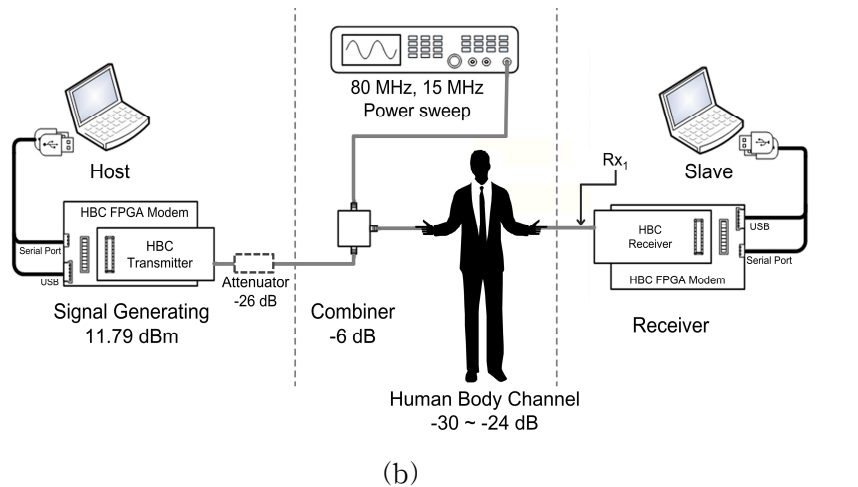


Figure 2.17 Diagram of measurement setup for BER evaluation according to the interference power (a) attenuator channel, (b) human body channel

For the in-band interference signal, the transmitted signal was directly connected to the power combiner without the attenuator. The signal loss of the attenuator channel was set to -24 dB that is equal to the measured average path loss of the human body channel. The attenuation of the human channel was determined by the subject through the average of the repeatedly measured values of the magnitude of the output signal versus the signal input to the human body channel. The total signal loss in the human channel is assumed to be -54 dB, including the attenuator that attenuate the output signal of the Tx module and the signal loss of the human channel, combiner in the mobile environment. Fig. 2.17 shows the measurement setup for BER evaluation versus SIR. The experiments were performed through both the attenuator and the human body channel by increasing the interference power for the out-of-band and in-band interference.

2. Performance and test results

A) Receiver

A transceiver module that transmits data through the human body channel using the FSDT modulation was developed [2]. The FSDT scheme transmits digital data using Walsh 64 code without analog modulation. Therefore, the transmitted signal was expressed as a non-return-to-zero(NRZ) code containing clock information. At a receiver, a clock signal was recovered from the received NRZ signal by a clock and data recovery circuit. The swing range of the clock signal commonly specified relative to the rail voltages. in this study case, the clock signal has the amplitude of 3.3 V and a clock frequency of 32 MHz [2]. A full-swing clock signal generates switching noise, which causes ground bounce. Ground bounce noise affects the signal received at the input terminal of the receiver through substrate coupling. The ground bounce noise caused by clock switching has the same frequency component as the received signal, and its amplitude corresponds to or is larger than that of the received signal due to the signal loss experienced through the channel. As a result, the ground bounce generated from the clock signal causes the sensitivity of the FSDT receiver to degrade; however, the generated ground bounce can be rejected by a differential scheme that is implemented with additional circuitry. In this thesis, to improve the performance of the HBC receiver, ground bounce is eliminated by differential to single circuitry added to the receiver AFE. Figure 2.18 shows the additional circuitry for rejecting ground bounce.

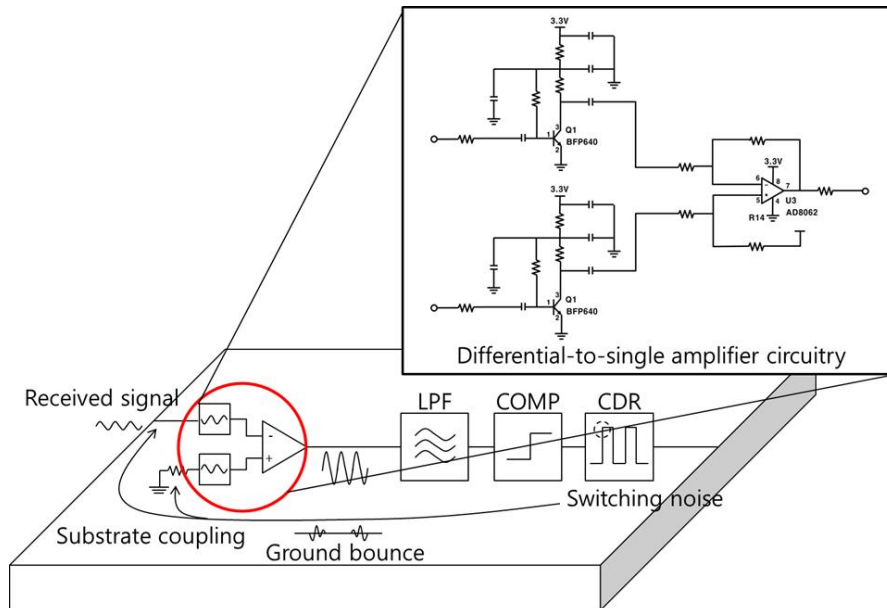


Figure 2.18 HBC receiver and differential to single circuitry

A differential to single amplifier comprises two single-ended amplifiers that are connected as a source coupled pair. The differential to single amplifier rejected the common mode noise. The proposed HBC receiver has a sensitivity of $165 \mu\text{V}_{\text{pp}}$ by rejecting the common mode noise and a dynamic range of 91.1 dB, from $165 \mu\text{V}_{\text{pp}}$ to $3.3 \text{ V}_{\text{pp}}$. This result shows that the proposed HBC receiving module can receive signals even with a signal loss of -9.1 dBm compared to [2]. The implemented receiver is capable of over -90 dB signal loss, hence it can be used for wearable and implantable devices.

B) BER versus interference frequency

The measured BER curves for the FSMT modulation is compared with that of the correlation-based modulation in [8] for interference frequencies from 1 MHz to 100 MHz, as shown in Figure 2.19.

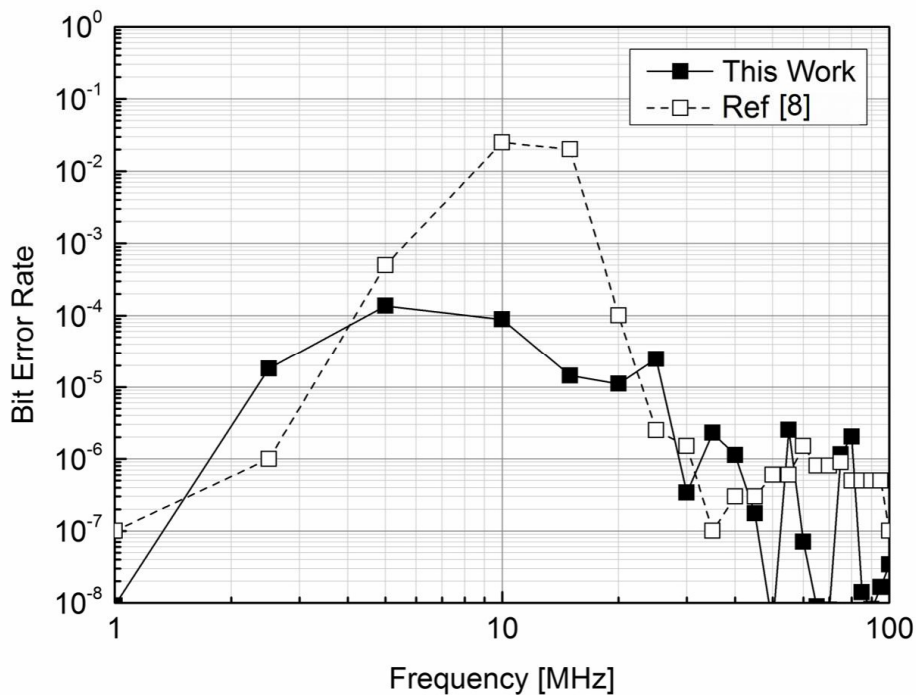


Figure 2.19 BER measurements under in-band and out-of-band interference of HBC

The FSDT scheme has a maximum bit error rate of 10^{-4} , which is introduced by the in-band interference from 8 MHz to 22 MHz. With the spread spectrum scheme, the FSDT modulation is robust against in-band interference signals; therefore, it has lower error rates than the correlation-based modulation. Under out-of-band interference signals above 30 MHz, including 80 MHz with a high PSD, the FSDT modulation shows low bit error rates of less than 10^{-5} . The BER curve for FSDT drops steeply by 10^{-5} in the interference frequency band above 25 MHz. This causes the structure of the FSDT receiver to remove high-frequency interference signals, similar to an active high-pass filter with limited bandwidth or a comparator with hysteresis. The BER curve for the FSDT modulation under out-of-band interference shows fluctuations; however, it is similar to the results of the correlation-based modulation.

C) BER versus SIR

The BER performances according to the interference power at both out-of-band interference of 80 MHz and in-band interference of 15 MHz were evaluated using the measurement setup shown in Figure 2.19 and Figure 2.20. Figure 2.19 shows a comparison of the BER performance of the FSDT modulation scheme against SIR at 80 MHz with that of AFH. AFH is a modulation method that avoids the interference signal when interference is present in the transmitted signal band [9]. As shown in Figure 2.20 a BER of 10^{-6} was obtained under the condition that the interference power is 28 dB larger than the signal power for both the attenuator channel and the human body channel.

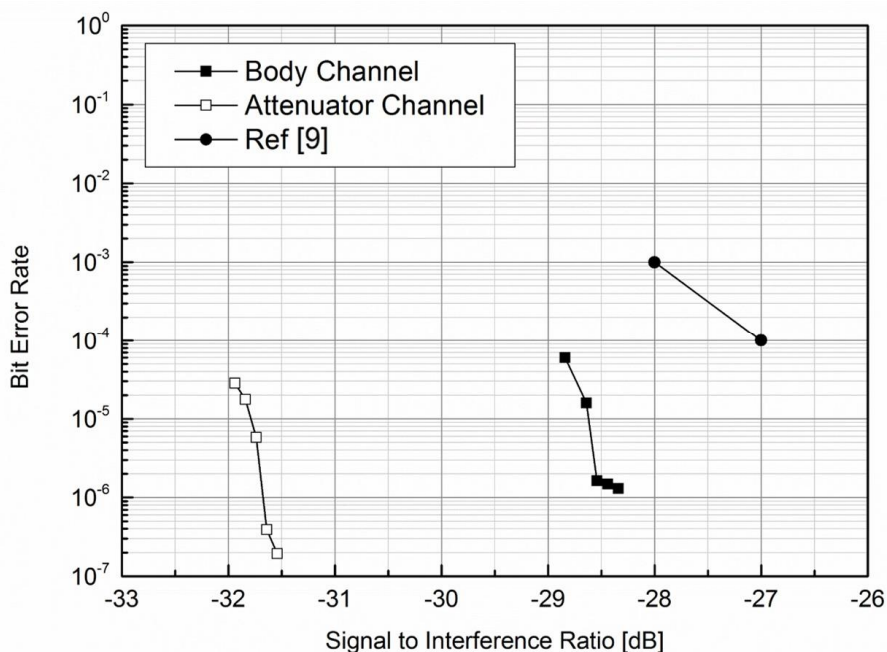


Figure 2.20 BER performance of the proposed FSDT receiver module at out-of-band of 80 MHz

The BER performance of the FSDT scheme was degraded by 3 dB of SIR in the human body channel compared with the attenuator channel. The degradation of BER performance is caused by the dispersive channel characteristics of the human body [6]. Compared with the previous study using AFH technique, the FSDT method improved the SIR by more than 5 dB for the attenuator channel and 2 dB for the human body channel at a BER of 10^{-4} . Figure 2.21 shows the BER performance versus SIR at in-band interference of 15 MHz.

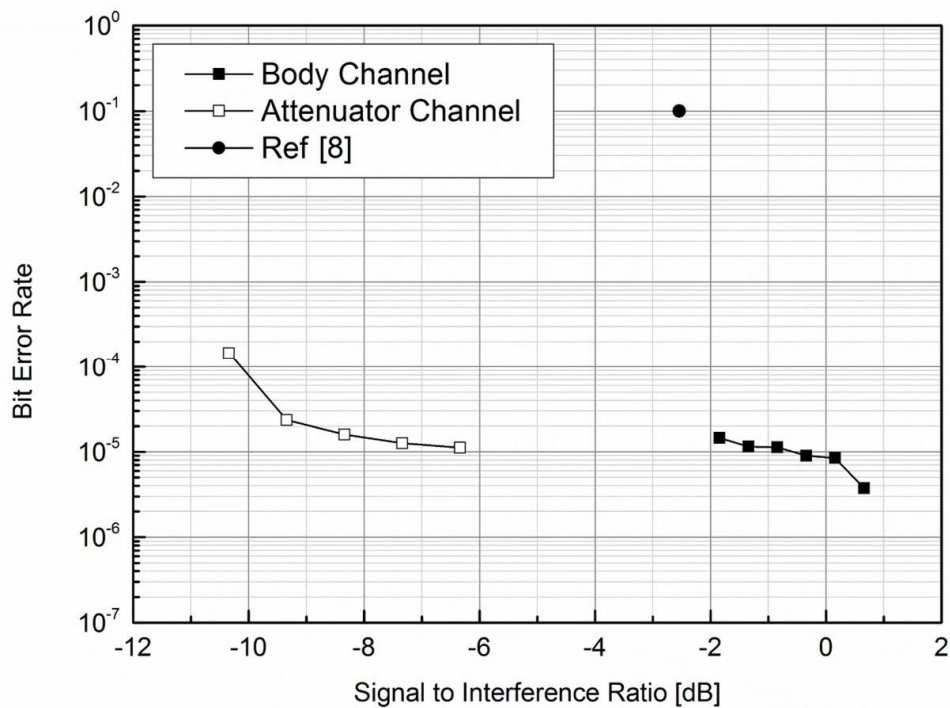


Figure 2.21 BER performance of the proposed FSDT receiver module at in-band interference of 15 MHz

As shown in Figure 2.21, SIR level at BER of 10^{-5} for the attenuator channel is approximately 3 dB lower than that for the human body channel. However, SIR level under in-band interference of 15 MHz is 26 dB higher than that under out-of-band interference of 80 MHz. This discrepancy comes from the

frequency response of the receiver structure. The low pass filter and the limited gain-bandwidth product of the amplifier in the receiver reject out-of-band interference. The FSDT modulation has 1,000 times lower error rate than the correlation-based scheme in [8] under similar SIR level of approximately -2.54 dB.

The FSDT modulation achieved a lower bit error without requiring a hopping technique to avoid the interference band, which would have increased circuit complexity. The performance of the proposed HBC module is compared with the methods in other studies, in Table 2.13.

Table 2.13 Performance comparison with conventional body channel transceiver

Parameters	This thesis	Chang [2]	Cho [8]	Fazzi [9]
Modulation scheme	FSDT	FSDT	AFH	Input clamping
Frequency band	8 MHz to 22 MHz	8 MHz to 22 MHz	30 MHz to 120 MHz	1 MHz to 30 MHz
Sensitivity	165 μ V _{pp} (-82.8 dBm)	262 μ V _{pp} (-73.7 dBm)	503 μ V _{pp} (-65dBm)	350 μ V _{pp}
Bit error rate	$< 10^{-6}$ 165 μ V _{pp}	$< 10^{-6}$ 250 μ V _{pp}	$< 10^{-5}$ 710 μ V _{pp}	$< 10^{-3}$ 450 μ V _{pp}
Data rate	2 Mbps	2 Mbps	10 Mbps	8.5 Mbps
BER @ 15 MHz with SIR of -2.54 dB	$< 10^{-4}$	NA	NA	$< 10^{-2}$
SIR @ 10^{-4} BER in 80 MHz interference	-28.84 dB	NA	-27 dB	NA

in this study, the BER performance of an HBC module using FSDT was evaluated under different interference conditions. Based on the antenna effect of the human body, the BER was measured in the FM frequency band, which is known to have a high PSD [9]. In addition, a continuous wave of 15 MHz was introduced as the in-band interference, which is the nearest frequency to the center of the modulated signal. As a result, the HBC transceiver using FSDT had a lower bit error rate than AFH and a correlation based module, under different interference conditions.

IV. Touch-based dual-transmission system

A. Applications of human body communication

Mobile devices are essential elements in everyday life. In recent years, a variety of new communication devices has become common, such as smart-phones, laptops, PDAs, and tablet PCs. These devices can use wired and/or wireless technologies for data transmission, enabling mobile devices to communicate with each other [18-22]. Wired data communication is capable of high-speed data transfer; however, it requires a dedicated cable, while wireless data communication requires a complex network setup procedure. To overcome these disadvantages, HBC is proposed [1]. HBC provides an intuitive and simple interface to communicate using the human body as a medium for communication [23-24]. This technology uses the human body as a transmission channel to transmit data between devices and allows users to choose an intuitive service rather than deal with the complexity of searching for and selecting each peripheral device. Moreover, as security studies on various communication methods have been carried out [25], HBC has the advantage of improved security owing to physical contact between the human body and the device [23]. HBC can be used to establish a network connecting mobile devices and printers, using multimedia applications [26 - 29], and HBC is standardized to IEEE 802.15.6 [11]. Despite continuous efforts to improve the data transmission rate of HBC, the data transmission rate remains low compared to that of wireless communication technologies. For transmitting high-capacity multimedia data using HBC, continuous contact with the devices is necessary. These requirements limit the behavior of users and prevent HBC from being used in some applications. Additionally, an algorithm is needed in case of loss of contact during data transmission. In this part, a touch-based dual-transmission(TBDT) application system, combined with WLAN, is proposed to overcome the disadvantages of HBC technology. The

proposed technology adds high data rates and mobility during data transmission to the existing HBC technology. Figure 3.1 shows the configuration of the TBDT application system.

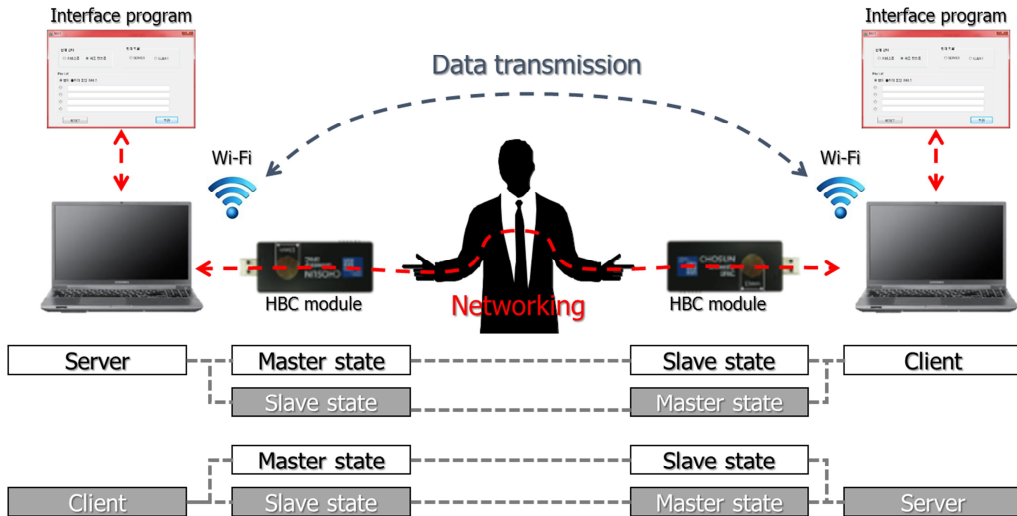


Figure 3.1 Touch-based dual-transmission communication system diagram

in this study, a dual-transmission application system is proposed that combines HBC for touch-based networking with a data transmission system using wireless-fidelity(Wi-Fi) direct and introduces the system configuration and a service scenario.

The proposed technology combines the advantages of HBC with those of wireless communication technologies. A comparison between TBDT communication and other communication services is shown in Table 3.1.

Table 3.1 Comparison of TBCDT service with various communication services

	NFC	RFID	HBC	Wi-Fi	TBCDT
Data rate	Poor (424 kbps)	Poor (40 kbps)	Good (10 Mbps)	Excellent (54 Mbps)	Excellent (54 Mbps)
Service area	Poor (10 cm)	Poor (7 to 15 cm)	Poor (touch)	Good (90 m)	excellent (touch+90 m)
Connection frequency	13.56 MHz	13.56 MHz	8 - 22 MHz	2.4 GHz	-
Set-up time	Excellent (0.1 s)	Excellent (0.1 s)	Excellent (1 s)	Fair (3 - 5 s)	Excellent (1 s)
Power consumption	Excellent -	Excellent -	Good (194.7 mW)	Poor (975 mW)	Poor (194.7+975 mW)
Security	Good	Poor	Excellent	Poor	Excellent
Accessibility	Excellent	Excellent	Excellent	Fair	Excellent
Feature	Full duplexing	Half duplexing	Need contact	Need access point	Easy networking

Short-range wireless technologies (such as radio frequency identification (RFID), near field communication(NFC), and HBC) can transmit data quickly, by contacting devices at a fraction of the distance, or by placing devices where the transmission distance is less than 1 m and the network is constructed for 1 s [19-20]. In particular, HBC technology allows users to

transmit data via direct contact with the user's body, enabling connections to be more intuitive. Due to these various advantages, touch-based communication technologies are applicable to various types of portable devices such as smart-phones, tablet PCs, laptops, and PDAs. However, these communication technologies place limits on devices and users during data transfers because the service area is less than 1 m. Even HBC, with a high transmission rate of 10 Mbps, is often required to transmit high-capacity data, and the user must continuously connect with the two devices [24]. On the other hand, wireless communication technologies such as Wi-Fi, worldwide interoperability for microwave access(WiMAX), and ultra-wideband(UWB) have the ability to transmit large amounts of data at a rate of 50 Mbps or more and have the advantage of providing service coverage areas of approximately 10 m [30]. Consequently, wireless communication technologies are applied to many portable devices.

Recently, wireless communication and HBC have been enhanced to increase data rates [31-32] and to reduce power consumption [33-34]. However, with wireless communication technologies, it is a more complicated task than with the touch-based communication technology to form a network between devices to communicate data. The TBDT communication system is proposed, which combines the advantages of HBC with wireless communication for broader service coverage and high data rates. Figure 3.2 shows the service coverage area and data rate of the TBDT communication system. The dual-transmission communications system combines HBC with wireless communication technologies to construct a network of wireless communication devices that forms a wider range of services than traditional HBC.

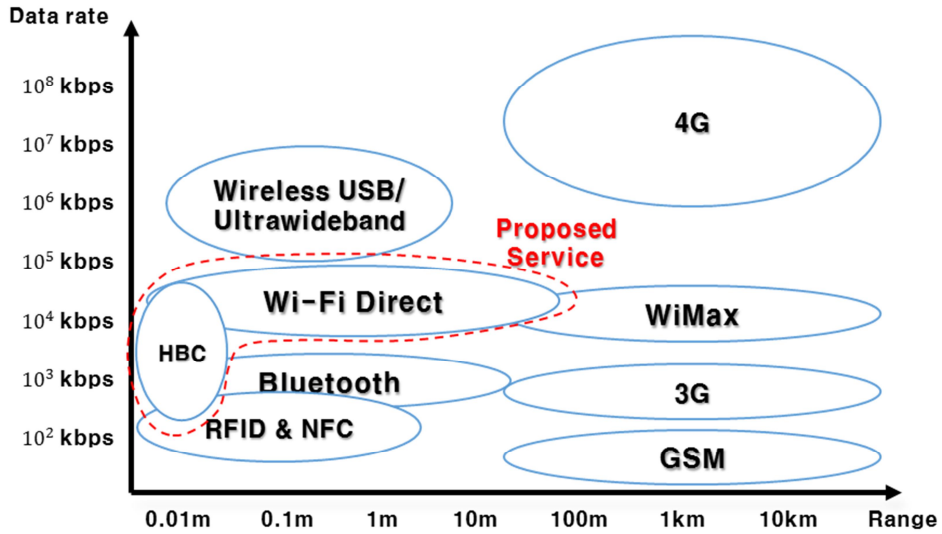


Figure 3.2 Touch-based dual-transmission communication service coverage area

This system can provide networking with simple touch without a separate complex configuration procedure. The data is transmitted via the WLAN network, enabling convenient and intuitive service delivery without restrictions on the movements of the users.

B. System configuration of dual-transmission application system

1. Physical signaling

HBC technology has been studied by many research groups. The HBC design proposed by Zimmerman at MIT has a 33 kHz operating frequency and a 2400 bps data rate [23]. FSDT was proposed to transmit data with less power without frequency modulation. A modem and analog front-end(AFE) with a data rate of 2 Mbps was developed using frequency selective spread code [35].

In the TBDT application system, HBC using the FSDT method is used. Table 3.2 shows the specifications of the HBC module.

Table 3.2 Specifications of HBC module

	Specifications
Modulation	Frequency Selective Digital Transmission
Duplexing	Time Division Duplexing
Frequency	8 - 22 MHz
Power supply	3.3 V
Power consumption	194.7 mW
Size	34 mm × 87 mm
Electrode type	Metal electrode, Transparent electrode

A prototype board for the TBDT application system is assembled, and it is composed of a field programmable gate array(FPGA) board that implements the FSDT method, a processor interface program for connecting the FPGA board, an AFE, and an AFE receiver. The prototype board is designed with a

universal serial bus(USB) as a host interface. The size of the prototype board is 30 × 70 mm, and the board is powered via USB to 5 V. The 5 V power via USB is converted to 3.3 V, which is supplied to the prototype board. Figure 3.3 shows the metal electrode HBC module and transparent electrode HBC module.



Figure 3.3 Metal electrode HBC module and transparent electrode HBC module

With the growing popularity of smart-phones, the input devices are being replaced with by touch screens. A metal electrode HBC module using a touch screen interface is limited to smart-phone and tablet PC applications, for which these components are very important in the design. On the other hand, transparent electrodes are easy to apply to touch screens and to combine with display devices using various types of electrodes. Further, the transparent electrode module with a size of 22 × 48 mm is larger than the metal electrode module with a diameter of 15 mm. The level of the received signal was directly proportional to the size of the transmitted electrode [36]. Because the application of the conductive transparent electrode allows the use of a transmission electrode of the whole size of the display, the received signal level is increased without increasing the transmitting signal power, thereby improving the rate of communication and enabling more reliable communication.

2. Network setup

HBC uses time-division duplexing(TDD) of a half-duplex communication channel to form the network for a dual-transmission application system. Although there are various types of data communication systems using the half-duplex communication method, the dual-transmission application system uses the master/slave method. Figure 3.4 shows the state diagram of the network setup.

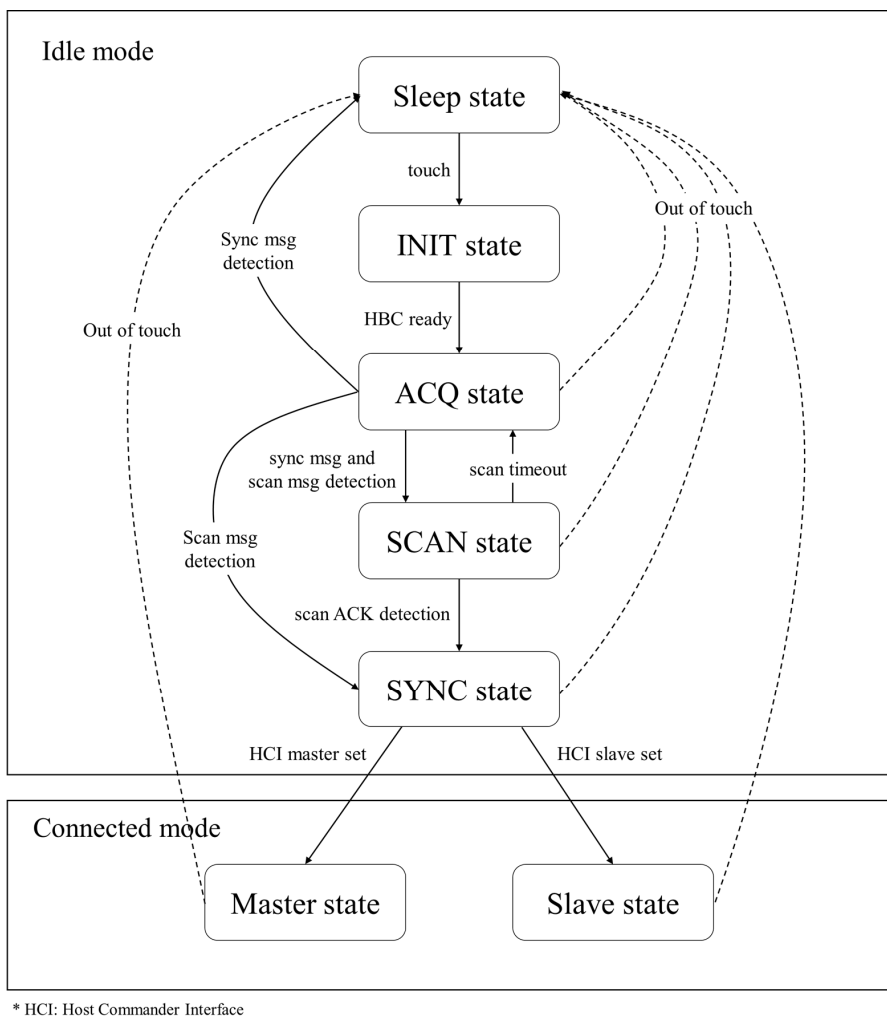
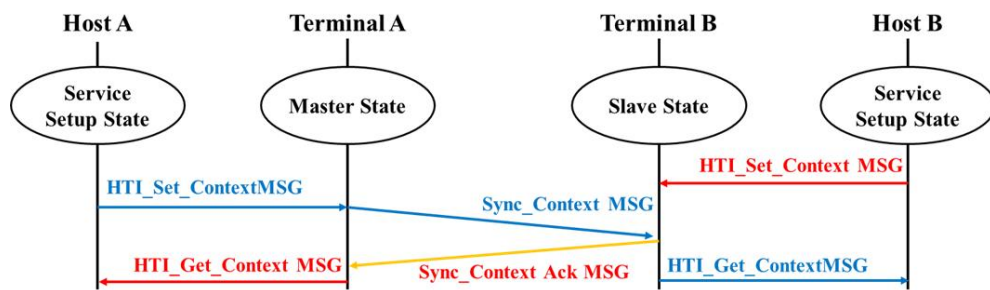


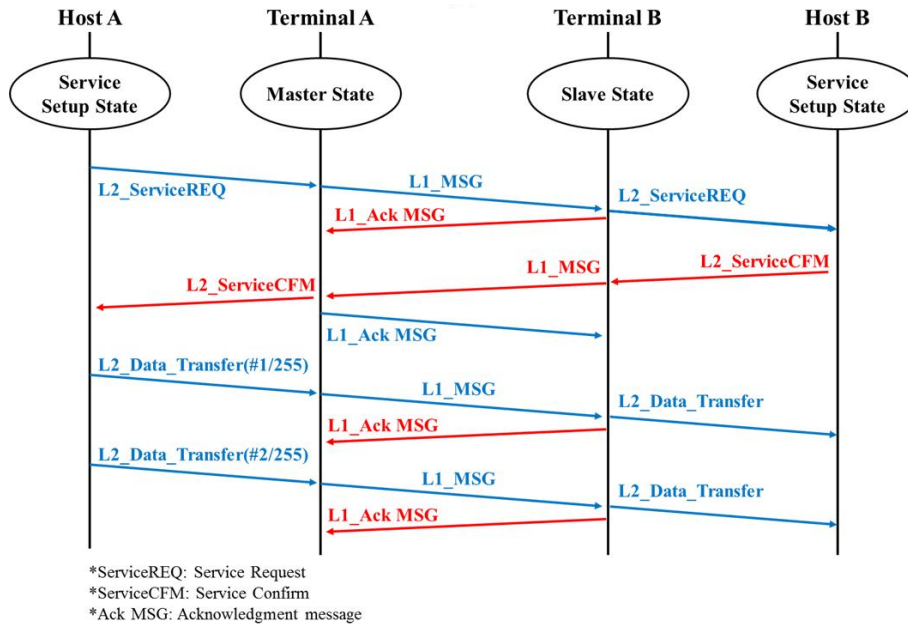
Figure 3.4 Network layer state diagram

If contact is detected in the HBC module for network formation, the data is transmitted to the Initial state from the Sleep state, and the data is transmitted to the acquisition(ACQ) state for confirming the setup of the master/slave device after initialization of the device. Beacon signals from other HBC modules are detected for 100 ms while in the ACQ state. If the beacon signal is detected, it goes to the scan state and sets up the slave state. If the signal is not detected for 100 ms, it switches to the master state. If the HBC module is set to slave only, the beacon signal will not be detected, and the HBC module will be moved to the sleep state.

Protocols are defined for network formation using HBC. For this purpose, context info is defined as 4-byte data including the device information. The frame length is 10 ms, and the network transport ratio is defined as 5:5. The sub-framework for data transfer consists of lock time, preamble, beacon, header, and data, and this framework length is under 5 ms. Figure 3.5 shows the ladder diagram for the system setup.



(a)



(b)

Figure 3.5 (a) Network setup, (b) Data transmission ladder diagram

The system consists of host A of the master role, terminal A of the master state, host B of the slave role, and terminal B of the slave state. The process of forming a network between the master and the slave is as follows. Each host transmits a message(HTI_Set_Context MSG), which contains context info at the terminals of the current state, to transmit information on the current situation. The terminal accepts the HTI_MSG and sends a Sync_Context_MSG containing the master status of the host. The slave, after receiving the Sync_Context_MSG, will send the Sync_Context_ACK_MSG to the master, including context Info.

Upon successful completion of this process, each terminal will send context info including status of the master and slave to each host through an HTI_Get_Context_Info_MSG. Each of the hosts determines the services according to the context info of the two pieces of equipment via the context info from the side of the receiving device. It takes about 145 ms to form a network.

3. Data transfer

When the network is established for data transfer using HBC, the HBC transmitter and receiver modules will be set to the master and slave, respectively, and then, multimedia devices will be set to the server and client, respectively. At this point, the master acts as the AP for the network connection and the method connecting the slave device to the master device is used. The server performs the user contents transfer, and both the master and the client can act as both servers and clients. The dual-transmission application system uses wireless communication between the server to provide user contents and the client to use the contents. In this study, Wi-Fi direct is used to form the data transfer channel, as it is the most common and fastest wireless communication technology currently available. The server for data transfer acts as a Wi-Fi direct Server by activating Wi-Fi direct on all the devices. Moreover, when the client device receives data for the network connection through HBC, it senses the signal for the Wi-Fi server from the activation of the Wi-Fi direct device, and forms the network between the Wi-Fi server and client. After the network is formed, the user is preset in the master and slave functions to provide the contents. Data transmission of devices set to master and slave provide service offering contents to the client from the server. Data transmission between devices is set to master, and thus, the master can be selected once again in the case of devices between servers and clients. If two devices set to the slave are connected, one device must be reset to the master because it is impossible to connect two slaves to each other, and the server must be turned into a master. After creating a network, devices form server and client states according to the user's choices. At this time, each host transfers its status to the server through the HTI_Set_Context MSG. The server and the client send the data to the other party through the Sync_Context_MSG, and they determine the service through context info. Through this process, user contents are communicated.

4. System configuration

In the system diagram of the TBDT application system, the system consists of HBC modules to form the network, a laptop for the server, a client role, and a Wi-Fi direct system for transmitting user contents. The HBC module is a USB dongle-type device with electrodes for transmitting and receiving signals through human contact. The HBC module exhibits intuitive and intentional characteristics through electrodes for human contact. In addition to considering smart devices using a touch screen, HBC modules are designed with transparent electrodes of 22 x 48 mm in size, as shown in Figure 3.3 The metal electrodes, which have the characteristic of reducing signal power, are smaller in size for use with mobile devices. However, the transparent electrode, which is larger than its metal electrode counterpart, is easily used in devices with touch screens; moreover, the signal power of the transparent electrode module can be increased.

C. Performance evaluation of dual-transmission application system

The TBSDT application system, using HBC and wireless communications, adds convenience to one's lifestyle. The service areas of existing HBC technology support only the touch area. However, the TBSDT service is a system that can expand the service area through HBC by forming a network and connecting other devices, and by employing various communication methods. Through the transmission of NetworkID using HBC, this system replaces bluetooth pairing, and it can provide greater service coverages. The TBSDT system facilitates convenient communication between portable devices by forming a network through simple touch. In particular, it is possible to provide personalized network services by using a smart phone, which is the center of multimedia devices. For example, the user can watch videos on TV from videos played on the user's smart phone by touching the electrode on the smart phone. In addition, while watching videos on TV, the user can re-watch the videos on his or her smart phone by re-touching the electrode on the smart phone to disconnect the network. Authentication and network setup information is transmitted by touching devices; once the network is formed via new devices using HBC, existing networks can be cut off and connected to new devices based on a point-to-point network.

For providing the TBSDT application system, a service scenario is proposed. Figure 3.6 shows the flow chart of the service scenario.

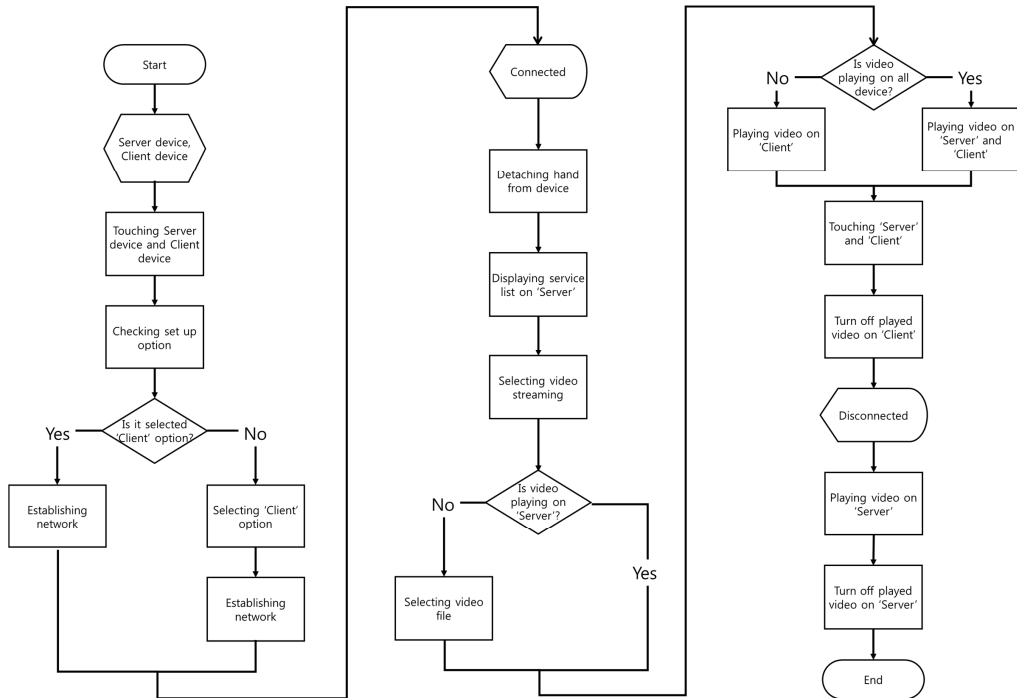


Figure 3.6 Scenario flow chart

The servers, such as smart-phones, laptops, and tablets are set to master, while the client device, such as the monitor or TV, is set to slave. Devices used as a server can also be used as client devices. When creating a network between the server and the client, the server device can form the network, set to the client device. To start the TBDT application system, the user contacts the server and client devices. The network is formed by confirming the server and client setup of each device. If the setup of the server and the client is set to server, the network is formed between server and client through changing to client from server. When the network is formed between the server and the client, the user selects the services after disconnection of the devices.

in this study, video streaming service is proposed using a TBDT application system. Video streaming services provide services for playing video clips from the server on the client. Videos played on the server play

continuously on the client. A while after the video streaming service, the service is terminated. Alternatively, the user can terminate the services intentionally by touching the HBC modules to disconnect the network between the server and the client. Figure 3.7 shows an illustration of the TBDT application system.



Figure 3.7 Touch-based dual-transmission communication service demonstration

IV. Conclusion

In HBC, it was confirmed that signal transmission characteristics are changed by various parameters due to the nature of human body. The characteristics of time delay can be analyzed through signal loss according to human body characteristics. When the signal is transmitted from the human chest to the wrist, the human body channel can be confirmed to be most suitable to use the HBC over the 60 MHz or more band which shows a characteristic of a small variation of the received signal. Also, the average time delay is about 225 in each transmission and reception direction, and the RMS delay is about 145 in each cases. The correlations between body composition and signal loss showed that the correlation between skeletal muscle and signal loss had a weak linear relationship of less than 0.3, so that it did not affect HBC more than body weight, body fat mass and total body water characteristics. In addition, correlation analysis between body composition and signal loss revealed that the correlation between skeletal muscle and signal loss has a weak linear relationship of less than 0.3, so that it has no significant effect on HBC than body weight, fat mass and total body water characteristics. Considering such channel characteristics, transmitter and receiver modules are expected to help design wearable HBC devices.

Under the interference condition examined, the FSDT had lower error rate than other modulation schemes because its BER is less than 10^{-4} for in-band interference and less than 10^{-5} for out-of-band interference. The FSDT method has -21.34 dB SIR levels at a BER of 10^{-5} in human body channel at 80 MHz for out-of-band interference. As shown by the BER in the 15 MHz and 80 MHz interference bands, in-band interference more affects HBC than out-of-band interference. These results show that the HBC using FSDT has robust characteristics in 80 MHz out-of-band interference band. The BER performance of the FSDT, which is based on IEEE 802.15.6, was analyzed for

the first time. This result shows that the HBC using FSDT has a 100 times lower error rate at the center frequency of the FSDT than other modulation schemes. In these results, an FSDT method with improved sensitivity was able to increase reliability. This system is suitable for organizing a BAN.

High frequency RFID , which uses the 13.56 MHz frequency band, is used for tasks, such as tagging goods and the mass transportation of goods [18]. NFC is mainly used for data transmission, such as authentication and payment in mobile devices, such as smartphones [19]. These short-range WLAN are not suitable for transmitting multimedia data, because they are used to transmit a few Kb of data over a short-range. In addition, devices must be very close each other to establish a network between them via the short-range system. Although it can be used for network connection through the lead range extension of the short-range WLAN, an additional authentication procedure is needed to select the network when there are many servers and client devices nearby. As the TBDB system connects the network via HBC, the devices do not need to be physically close to each other. The demonstration in Figure 3.7 shows the advantage of intuitively selecting the server and client, because the user directly touches the devices to connect to the network. Wi-Fi direct can transmit a large amount of data at a speed of over 50 Mbps over a distance of 90 m [30]. Wi-Fi direct searches for devices in the lead range and then connects them through the authentication process. Wi-Fi direct have a complicated connection process for obtaining connectivity between different types of devices. In addition, wired communication has the disadvantage of requiring compatibility between the device port and the connector. The TBDB application system overcomes these shortcomings by providing a high data rate, large range-of-service, and a wireless communication system that users can activate with an easy and intuitive touch to form the network. The TBDB system provides intuitive and convenient service and a high-speed data communication system through simple touch by combining HBC and wireless communication. This system enables data communication at a transmission speed of 50 Mbps through

Wi-Fi direct by forming a network for data communication within 1 s through intuitive touch using HBC technology. It can overcome the problems of HBC, which require constant contact maintenance with relatively low transmission speed and the problems of WLAN, which require a complicated authentication process. Through such a system, it is possible to transmit and receive data at high speed through a simple human touch connection between various devices, so that contents can be shared easily. In the future, we expect that it will be possible to form one or many networks and to provide various communication services by studying to improve the reception performance of HBC and reducing power consumption.

Reference

- [1] T. G. Zimmerman, "Personal Area Networks: Near-field intrabody communication," *IBM systems J.*, vol. 35, no. 3.4, pp. 609-617, 1996.
- [2] C. H. Hyung, S.-W. Kang, S. O. Park, and Y. T. Kim, "Transceiver for human body communication using frequency selective digital transmission," *ETRI J.*, vol. 34, no. 2, pp. 216-225, 2012.
- [3] C. K. Ho et al., "High bandwidth efficiency and low power consumption walsh code implementation methods for body channel communication," *IEEE Trans. Microw. Theory Tech.*, vol. 62, no. 9, pp. 1867-1878, 2014.
- [4] C. H. Hyung, J. H. Hwang, S. W. Kang, S. O. Park, and Y. T. Kim, "A feasibility study on the adoption of human body communication for medical service," *IEEE Trans. Circuits Syst. II Express Briefs*, vol. 62, no. 2, pp. 169-173, 2015.
- [5] N. Cho, J. Yoo, S. J. Song, J. Lee, S. Jeon, and H. J. Yoo, "The human body characteristics as a signal transmission medium for intrabody communication," *IEEE Trans. Microw. Theory Tech.*, vol. 55, no. 5, pp. 1080-1085, 2007.
- [6] J. H. Hwang, T. W. Kang, Y. T. Kim, and S. O. Park, "Measurement of transmission properties of HBC channel and its impulse response model," *IEEE Trans. Instrum. Meas.*, vol. 65, no. 1, pp. 177-188, 2016.
- [7] T. W. Kang, K. Oh, J. H. Hwang, S. Kim, H. Park, and J. Lee, "Measurement and analysis of electric signal transmission using human body as medium for WBAN applications," *IEEE Trans. Instrum. Meas.*, vol. 67, No. 3, pp. 527-537, 2018.
- [8] A. Fazzi, S. Ouzounov, and J. van den Homberg, "A 2.75 mW wideband correlation-based transceiver for body-coupled communication," in *Solid-State Circuits Conference-Digest of Technical Papers, ISSCC 2009*. pp. 204-205, 2009.
- [9] N. Cho, L. Yan, J. Bae, and H. J. Yoo, "A 60 kb/s/10 Mb/s adaptive frequency hopping transceiver for interference-resilient body channel communication," *IEEE J. Solid-State Circuits*, vol. 44, no. 3, pp. 708-717, 2009.

- [10] K. Oh, T. W. Kang, S. Kim, H. Park, I. Lim, and S.-W. Kang, "Low-noise inducing Rx for human body communication," *IET Electron. Lett.*, vol. 52, no. 21, pp. 1740-1742, 2016.
- [11] IEEE Standards Association, *IEEE Standard for Local and metropolitan area networks - Part 15.6: Wireless Body Area Networks*, no. February. 2012.
- [12] C. H. Hyung, Y. T. Kim, J. H. Hwang, and K. H. Park, "Energy harvesting from ambient electromagnetic wave using human body as antenna," *Electron. Lett.*, vol. 49, no. 2, pp. 149-151, 2013.
- [13] J. H. Hwang, T. W. Kang, Y. T. Kim, and S. O. Park, "Analysis on co-channel interference of human body communication supporting IEEE 802.15.6 BAN standard," *ETRI J.*, vol. 37, no. 3, pp. 439-449, 2015.
- [14] J. H. Hwang, T. W. Kang, C. H. Hyung, and S. O. Park, "Bit error rate degradation model for time-delay parameter of co-channel interference occurring in human body communication," *IET Commun.*, vol. 37, no. 3, pp. 724-733, 2016.
- [15] J. H. Hwang, T. W. Kang, J. H. Kwon, and S. O. Park, "Effect of Electromagnetic Interference on Human Body Communication," *IEEE Trans. Electromagn. Compat.*, vol. 59, no. 1, pp. 48-57, 2017.
- [16] M. A. Callejon, D. Naranjo-Hernandez, J. Reina-Tosina, and L. M. Roa, "A comprehensive study into intrabody communication measurements," *IEEE Trans. Instrum. Meas.*, vol. 62, no. 9, pp. 2446-2455, 2013.
- [17] Martin, A. D., Daniel, M. Z., Drinkwater, D. T., & Clarys, J. P. "Adipose tissue density, estimated adipose lipid fraction and whole body adiposity in male cadavers." *International journal of obesity and related metabolic disorders: journal of the International Association for the Study of Obesity*, vol. 18, no. 2, pp. 79-83, 1994.
- [18] R. Weinstein, "RFID: A technical overview and its application to the enterprise," in *IT Professional*, vol. 7, no. 3, pp. 27-33, 2005.
- [19] V. Coskun, B. Ozdenizci, and K. Ok, "A survey on near field communication (NFC) technology," *Wireless Personal Communications*, vol. 71, no. 3, pp. 2259-2294, 2013.
- [20] Bluetooth Special Interest Group, "Bluetooth core specification version 4.2," *Bluetooth Core Specif. Version 4.2*, December, p. 2684, 2014.

- [21] IEEE, "IEEE 802.11," IEEE Std 802.11-2012 (Revision of IEEE Std 802.11-2007), vol. 2012, March. pp. 2793, 2012.
- [22] S. Maity, D. Das, X. Jiang, and S. Sen, "Secure human-internet using dynamic human body communication," in Proceedings of the International Symposium on Low Power Electronics and Design, 2017.
- [23] D. G. Park, T. K. Kim, S. T. Bong, J. H. Hwang, C. H. Hyung, and S. W. Kang, "Context aware service using intra-body communication," in Proceedings - Fourth Annual IEEE International Conference on Pervasive Computing and Communications, PerCom 2006, vol. pp. 84-91, 2006.
- [24] D. G. Park, J. K. Kim, J. B. Sung, J. H. Hwang, C. H. Hyung, and S. W. Kang, "TAP: touch-and-play," Proc. ACM CHI 2006 Conf. Hum. Factors Comput. Syst., vol. 1, pp. 677-680, 2006.
- [25] M. La Polla, F. Martinelli, and D. Sgandurra, "A Survey on Security for Mobile Devices," IEEE Commun. Surv. Tutorials, vol. 15, no. 1, pp. 446-471, 2013.
- [26] R. Negra, I. Jemili, and A. Belghith, "Wireless body area networks: applications and technologies," in Procedia Computer Science, vol. 83, pp. 1274-1281, 2016.
- [27] M. Patel and J. Wang, "Applications, challenges, and prospective in emerging body area networking technologies," IEEE Wirel. Commun., vol. 17, no. 1, pp. 80-88, 2010.
- [28] H. Cao, V. Leung, C. Chow, and H. Chan, "Enabling technologies for wireless body area networks: A survey and outlook," IEEE Commun. Mag., vol. 47, no. 12, pp. 84-93, 2009.
- [29] J. F. Zhao, X. M. Chen, B. D. Liang, and Q. X. Chen, "A review on human body communication: signal propagation model, communication performance, and experimental issues," Wirel. Commun. Mob. Comput., 2017.
- [30] D. Camps-Mur, A. Garcia-Saavedra, and P. Serrano, "Device-to-device communications with WiFi direct: Overview and experimentation," IEEE Wirel. Commun., vol. 20, no. 3, pp. 96-104, 2013.
- [31] C. C. Chung, C. T. Chang, and C. Y. Lin, "A 1 Mb/s-40 Mb/s human body channel communication transceiver," in 2015 International Symposium on VLSI Design, Automation and Test, VLSI-DAT, 2015.

- [32] H. Cho et al., “A 79 pJ/b 80 Mb/s full-duplex transceiver and a 42.5 μ W 100 kb/s super-regenerative transceiver for body channel communication,” *IEEE J. Solid-State Circuits*, vol. 51, no. 1, pp. 310-317, 2016.
- [33] J. Bae, K. Song, H. Lee, H. Cho, and H. J. Yoo, “A 0.24-nJ/b wireless body-area-network transceiver with scalable double-FSK modulation,” *IEEE J. Solid-State Circuits*, vol. 47, no. 1, pp. 310-322, 2012.
- [34] S. Anand Gopalan, “Energy-efficient MAC protocols for wireless body area networks: Survey,” *Int. Congr. Ultra Mod. Telecommun. Control Syst.*, pp. 739-744, 2010.
- [35] H. Il Park, I. G. Lim, S. Kang, and W. W. Kim, “Human body communication system with FSBT,” in *Proceedings of the International Symposium on Consumer Electronics, ISCE*, 2010.
- [36] K. Fujii and K. Ito, “Evaluation of the received signal level in relation to the size and carrier frequencies of the wearable device using human body as a transmission channel,” in *IEEE APS 2004*, vol. 1, pp. 105-108.

List of Publications

Paper

1. **Kunho Park**, Min Joo Jeong, Jong Jin Baek, Se Woong Kim, and Youn Tae Kim, "BER performance of human body communications using FSMT", IEICE Trans. Commun., vol. E102-B, no. 3, pp 522-527, Mar. 2019.
2. **Kunho Park**, Jong Jin Baek, Se Woong Kim, Min Joo Jeong, and Youn Tae Kim, "Touch-based dual-band system combined human body communications and wireless LAN for wearable devices", Electronics, vol. 8.3, no. 335. pp. 1-11, Mar. 2019.
3. **Kunho Park**, Jong Jin Baek, Se Woong Kim, Min Joo Jeong, and Youn Tae Kim, "Analysis on frequency-dependency of conductive signal transmission channel for wearable devices", submitted to IEICE Electronics Express, Jan, 2019.
4. Min Joo Jeong, **Kun Ho Park**, Jung Hwan Hwang, Chang Hee Hyung, Sung Weon Kang, and Youn Tae Kim, "Feasibility study on application of power transmission using magnetic coupling to body area network", Electronics Letters, vol. 48, no. 16, pp. 1013-1015, 2012.
5. Min Joo Jeong, **Kun Ho Park**, Jong Jin Baek, Se Woong Kim, and Youn Tae Kim, "Wireless charging with textiles through harvesting and storing energy from body movement", Textile Research Journal, vol. 89 no. 3, pp. 347-353, 2019.

6. Jong Jin Baek, Se Woong Kim, Kun Ho Park, Min Joo Jeong, and Youn Tae Kim, “Design and performance evaluation of 13.56-MHz passive RFID for E-skin sensor application”, IEEE Microwave and Wireless Components Letters, vol. 28, no. 12, pp. 1074-1076, 2018.

List of Publications

Conference

1. Kun Ho Park, Chang Hee Hyoung, Sung Weon Kang, and Youn Tae Kim, “Analog front end with improved sensitivity and evaluation on SIR for human body communication”, IEEE International Symposium Antennas and Propagation Society, July 2012
2. Kun Ho Park, Min Joo Jeong, Jong Jin Baek, Chang Hee Hyoung, Jung Hwan Hwang, and Youn Tae Kim, “Touch based multi-band service using human body communications”, IEEE International Symposium Antennas and Propagation Society, July 2013
3. Kun Ho Park, Jong Jin Baek, Jang Hyun Lee, and Youn Tae Kim, “Conductive power transmission with human body communication for implantable devices”, International biomedical engineering conference, Nov. 2014
4. Min Joo Jeong, Kun Ho Park, Jang Myoung Kim, Jung Hwan Hwang, Chang Hee Hyoung, and Youn Tae Kim, “Wireless power transmission on surface of the human body using resonant coil of thin-film type”, IEEE International Symposium Antennas and Propagation Society, July 2013.

5. Min Joo Jeong, Tae Il Yun, Kun Ho Park and Youn Tae Kim, “Wireless power transmission using wearable coils for Ubiquitous healthcare”, International Biomedical Engineering Conference, Nov 2014.

6. Jang Hyun Lee, Kun Ho Park, Min Joo Jeong, Jong Jin Baek and Youn Tae Kim, “Analysis on frequency-dependency of conductive signal transmission channel for biosensor network”, IEEE sensors, pp 1-3, Nov 2016.

List of Publications

Patent

1. Youn Tae Kim, Kun Ho Park, Jang Myoung Kim, Min Joo Jeong, Chang Hee Hyoung, Jung Hwan Hwang, Sung Weon Kang, “Transmitting and receiving electrode system and power transmission method using the same”, Application(24 Apr, 2012, US 13/454,614), Registration(10 Feb, 2015, US 08952676)
2. Youn Tae Kim, Kun Ho Park, Jang Myoung Kim, Min Joo Jeong, Chang Hee Hyoung, Jung Hwan Hwang, Sung Weon Kang, “Phased spreading scheme-based transmission apparatus and method of operating the same”, Application(27 Apr, 2012, US 13/458,157), Registration(1 Jul, 2015, US 08767798)
3. Youn Tae Kim, Kun Ho Park, Jang Myoung Kim, Min Joo Jeong, Chang Hee Hyoung, Jung Hwan Hwang, Sung Weon Kang, “Spreading code producing apparatus”, Application(3 May, 2012, US 13/463,013), Registration(4 Aug, 2015, US 9100140)
4. Youn Tae Kim, Min Joo Jeong, Kun Ho Park, Jong Jin Baek, Janghyun Lee, Se Woong Kim, “Apparatus and method of charging mobile terminal using energy harvesting device”, (Nov 15, 2016, US 15/351,651)
5. Youn Tae Kim, Kun Ho Park, Jang Myoung Kim, Min Joo Jeong, Chang Hee Hyoung, Jung Hwan Hwang, Sung Weon

- Kang, “단계적 확산 방식 기반 송신 장치 및 그의 동작 방법”, Application(13 Mar, 2012, KOR 10-2012-0025457), Registration(21 Nov, 2013, 101333673)
6. Youn Tae Kim, Kun Ho Park, Jang Myoung Kim, Min Joo Jeong, Chang Hee Hyoung, Jung Hwan Hwang, Sung Weon Kang, “송수신 전극 시스템 및 이를 이용한 전력전송 방법”, Application(6 Apr, 2012, KOR 10-2012-0036072), Registration(26 Dec, 2013, 101347142)
 7. Youn Tae Kim, Kun Ho Park, Jang Myoung Kim, Min Joo Jeong, Chang Hee Hyoung, Jung Hwan Hwang, Sung Weon Kang, “체내 무선 전력 전송 시스템”, Application(16 Apr, 2012, KOR 10-2012-0039054), Registration(4 Feb, 2014, KOR 101360971)
 8. Youn Tae Kim, Kun Ho Park, Jang Myoung Kim, Min Joo Jeong, Chang Hee Hyoung, Jung Hwan Hwang, Sung Weon Kang, “확산 코드 발생 장치”, Application(April 20, 2012, KOR10-2012-0041460), Registration(4 Aug, 2014, KOR 1013609710000)
 9. Youn Tae Kim, Min Joo Jeong, Kun Ho Park, Jong Jin Baek, Janghyun Lee, Se Woong Kim, “에너지 하베스팅 소자를 이용한 휴대 기기의 충전 장치 및 방법”, (Mar 13, 2016, KOR10-2016-0032004)
 10. Youn Tae Kim, Kun Ho Park, Jong Jin Baek, Janghyun Lee, Se Woong Kim, “용량성 결합 방식을 이용한 무선 전력전송용 전극 및 이를 포함하는 의류”, (Nov 02, 2016, KOR10-2016-0144852)

Acknowledgement

I would like to thank my advisor, Professor Youn Tae Kim for his supervision, understanding, support, encouragement and personal guidance as I was working on this research and the thesis. I am deeply grateful to all of the professors from whom I have learned great deal of knowledge.

In addition, I have the deepest appreciation for the constructive criticism and excellent advice that provided by Prof. Keun-Chang Kwak, Dr. Jung Hwan Hwang, Prof. Hyun-Sik Choi and Prof. Eun Seo Choi and during the preparation of my thesis, as well as for their detailed review of the thesis after it was completed.

During this work, I collaborated with all my colleagues in the laboratory and I have great regard for all of them and wish to extend my sincerest thanks to all those in the Department of IT Fusion Technology who helped as I conducted my work.

My deepest thanks go to my family for all the care and support he has given me over many years. You are the best family in the world.

July 2019
Kunho park